

PHOTOCONDUCTIVITY AND LUMINESCENCE
IN Al_2O_3

By

BILLY GENE DRAEGER, JR.

Bachelor of Science

Oklahoma State University

Stillwater, Oklahoma

1975

Submitted to the Faculty of the
Graduate College of the
Oklahoma State University
in partial fulfillment of
the requirements for
the Degree of
MASTER OF SCIENCE
July, 1977

Thesis
1977
D758p
cop. 2



PHOTOCONDUCTIVITY AND LUMINESCENCE

IN Al_2O_3

Thesis Approved:

Gloss P. Sumner

Thesis Adviser

John G. Martin

R. E. Kumb

Norman M. Durbin

Dean of the Graduate College

989145

ACKNOWLEDGMENTS

The author wishes to express gratitude to Dr. Geoffrey P. Summers, his major adviser, for his guidance and help in the completion of this thesis and for maintaining an environment of professionalism in the work. Appreciation is also given to the other committee members, Dr. Joel J. Martin and Dr. Elton E. Kohnke for their valuable suggestions in the preparation of the final manuscript.

Thanks are given to the Physics Faculty of Oklahoma State University for the encouragement and fine instruction, Sister Jeanette Feldot for interesting discussions, and to Brenda Morrison for her excellence and efficiency in typing the thesis.

A special thanks is given to the author's God who gave an inward strength and guidance throughout the course of the work.

TABLE OF CONTENTS

Chapter	Page
I. INTRODUCTION	1
II. THEORY	3
Structure and Defects	3
Optical Density	5
Photoresponse	6
III. APPARATUS	10
Optical Density Measurements	10
Photoconductivity Measurements	10
Luminescence Measurements	16
Irradiations	18
IV. RESULTS AND DISCUSSION	20
Nominally Pure Sapphire	20
Non-Irradiated Sapphire	20
Electron-Irradiated Sapphire	23
γ -Irradiated Sapphire	23
Discussion of Nominally Pure Sapphire	27
Nominally Doped Sapphire	29
General Description of Samples	29
V^{3+} Doped Sapphire	29
Non-Irradiated Ruby	29
γ -Irradiated Ruby	32
Electron-Irradiated Ruby	37
Temperature Dependence of Irradiated Ruby	37
An Interesting Insaco Sample	41
V. FUTURE	47
A SELECTED BIBLIOGRAPHY	48

LIST OF FIGURES

Figure	Page
1. Structure of α - Al_2O_3	4
2. Apparatus for Measuring Photoresponse	11
3. Sample Assembly	13
4. Photon Flux as a Function of Wavelength	15
5. Apparatus for Measuring Luminescence	17
6. Spectral Dependence of Photoresponse for "As Received" Crystals of Al_2O_3	21
7. Optical Absorption Spectra of "As Received" Crystals of Al_2O_3	22
8. Spectral Dependence of the Photoresponse in Electron-Irradiated Al_2O_3 at 77 K and Room Temperature	24
9. Optical Absorption Spectrum of Electron- Irradiated Al_2O_3	25
10. Spectral Dependence of the Photoresponse of γ -Irradiated Al_2O_3 before and after a Bleach with 5.3 eV Light	26
11. Optical Absorption Spectra of Non-Irradiated and γ -Irradiated Al_2O_3	28
12. Optical Absorption of $\text{Al}_2\text{O}_3: \text{V}^{3+}$	30
13. Spectral Dependence of Photoresponse in Non- Irradiated Ruby and γ -Irradiated Ruby before and after a Bleach with 4.4 eV Light	31
14. Optical Absorption Spectra of Non-Irradiated and γ -Irradiated Ruby	33

Figure	Page
15. Difference Curve Between Optical Density Absorption Spectra of γ -Irradiated Ruby at Room Temperature before and after Bleaching for one hour with 4.4 eV Light	35
16. Photocurrent of γ -Irradiated Ruby at 4.4 eV as a Function of Time with no Bleaching and Bleaching with 4.4 eV Light	36
17. Spectral Dependence of Photoresponse in Non-Irradiated Ruby and Electron-Irradiated Ruby before and after a Bleach with 4.4 eV Light	38
18. Optical Absorption Spectra of Non-Irradiated Ruby and Electron-Irradiated Ruby before and after a Bleach with 4.4 eV Light	39
19. 4.5 eV Photoconductivity Bands in Ruby as Difference Curves	40
20. Optical Absorption Spectra of an Insaco Sample of Al_2O_3 before and after a Bleach with Light from a Deuterium Lamp	43
21. Emission Spectrum of Neutron-Irradiated Al_2O_3	44
22. Emission Spectrum of Non-Irradiated Insaco Sample of Al_2O_3	45

CHAPTER I

INTRODUCTION

The α form of corundum or $\alpha\text{-Al}_2\text{O}_3$ has some unusual properties. It is very resistive to radiation damage and corrosion. It also has a large compression strength (300,000 PSI for 99% pure Al_2O_3) and a melting point of about 2050°C. These properties make it difficult material to study. These properties also made corundum an appealing material for consideration for the inner walls of fusion reactors. However, recent experimental results indicate that other materials such as Y_2O_3 could be better suited.

It is generally agreed that an optical absorption band at 6.1 eV occurring in neutron, proton, and electron irradiated samples is produced by trapped negative charge located at an oxygen ion vacancy. Lee and Crawford (1) have suggested from optical bleaching experiments and polarized emission spectra that the 6.1 eV band is an F center (i.e., two electrons trapped at an oxygen ion vacancy), and another band at 4.8 eV is an F^+ center (i.e., a single electron trapped at an oxygen ion vacancy). These assignments have not yet been verified by further experiment.

Many of the 3d-group ions e.g., Fe^{3+} can enter the $\alpha\text{-Al}_2\text{O}_3$ lattice substitutionally for Al^{3+} ions. These substi-

tutional ions are usually found as accidental impurities in the material. Most of these ions have charge transfer transitions located in the region of the 6.1 eV band. Tippins (2) gives some of the charge transfer transition peaks around 6.1 eV as:

Ti^{3+} -6.9 eV

V^{3+} -5.75 eV

Cr^{3+} -6.94 eV

Fe^{3+} -6.38 eV

The Fe^{3+} also has a charge transfer peak at 4.8 eV.

Apart from some preliminary data obtained from neutron irradiated corundum (3), no detailed photoconductivity measurements on $\alpha\text{-Al}_2\text{O}_3$ have so far been reported. Several of the photoconductivity peaks that we have observed lie in the region about 5.9 eV.

A 5.35 eV optical absorption band in irradiated Al_2O_3 is believed to be due to Cr^{2+} impurity. Turner and Crawford (4) have concluded that this band is due to Cr^{2+} as a result of electron capture by the substitutional Cr^{3+} . Klabbley and Rose (5) have reported some high temperature thermoluminescence and esr experiments on electron irradiated Al_2O_3 which suggest that Cr^{4+} ions are formed. McClure (6) has indicated that both Cr^{2+} and Cr^{1+} are stable in corundum. On the evidence so far chromium seems to be an important impurity which is related to defect production and decay in corundum. We will present below a preliminary study of the effects of chromium ions on the photoconductivity of ruby and nominally undoped Al_2O_3 .

CHAPTER II

THEORY

Structure and Defects

The structure of $\alpha\text{-Al}_2\text{O}_3$ is illustrated in Figure 1. The structure is that of a hexagonal cell consisting of an equilateral triangle of oxygen atoms above and below an aluminum atom. The apexes of the top triangle are rotated through 60° relative to those of the bottom triangle. The aluminum atom sets along the line created by the centers of the triangles, but is displaced toward one of the triangles. The shortest Al-O distance in the cell is 1.86 \AA , and the longest Al-O distance in the cell is 1.97 \AA . The equilateral triangles give the cell 3 fold symmetry. The symmetry of the cell would be approximately C_{3v} , whereas the symmetry of the crystal is only C_3 because of the huge interstitial spaces in the crystal resulting from combining the cells.

There are several kinds of defect configurations possible in the corundum structure. A removal of an O^{-2} ion could result in F- type centers. F and F^+ centers would result if the site captured two electrons or one electron respectively. A removal of an Al^{3+} ion could result in V-type centers. V° and V^- centers would result if the site captured three or two holes respectively. $\text{V}^=$ centers would result

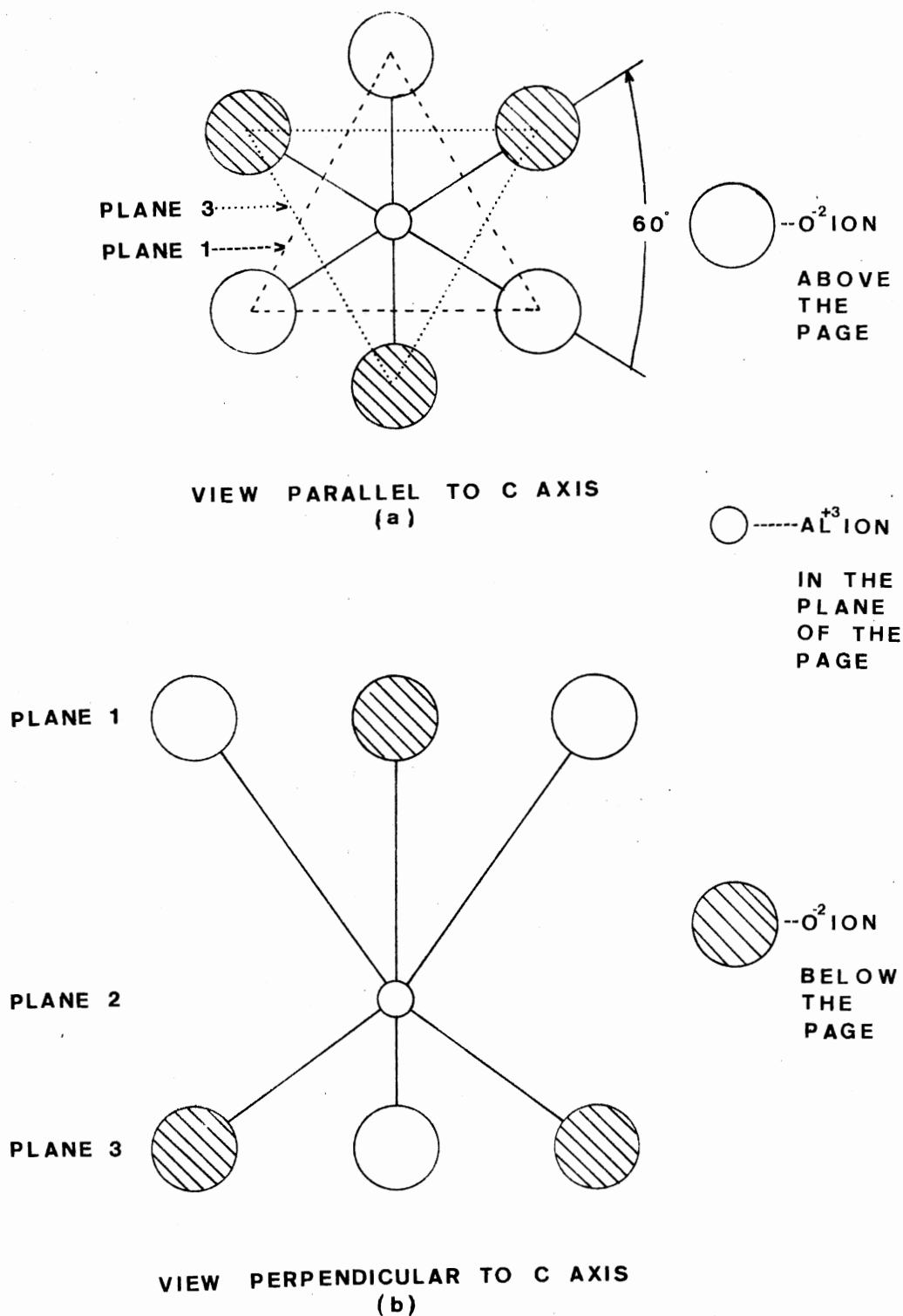


Figure 1. Structure of $\alpha\text{-Al}_2\text{O}_3$. Part a of the figure shows the C_{3v} symmetry of the cell. Part b of the figure shows the aluminum ion shifted toward one of the oxygen planes.

if one hole was captured by the site. A V_{OH}^- center is formed if an OH ion is adjacent to the V^- center. Turner and Crawford (7) suggest that the V_{OH}^- is an important contribution to a 3 eV optical absorption band in γ -irradiated Al_2O_3 .

Trivalent ions such as the transition metal ions Cr^{3+} , Fe^{3+} , V^{3+} , Ni^{3+} , Ti^{3+} and Mn^{3+} could enter substitutionally, for the Al^{3+} ion. Other charge states of these or other ions would need charge compensation.

Optical Density

Optical density is defined to be:

$$OD = \log\left(\frac{I_0}{I}\right)$$

where

I_0 is the intensity of light incident on the sample

I is the intensity of the light transmitted through the sample

The effect of reflections at the crystal surfaces are taken care of by subtracting the untreated sample's optical density from the optical density of the sample under investigation. The intensity of light transmitted by the crystal is related to the absorption coefficient, α , by the equation:

$$\frac{I}{I_0} = e^{-\alpha d}$$

where

d is the thickness of the crystal

Substitution of the intensity ratio into the definition of the optical density gives:

$$OD = \log(e^{\alpha d}) = \frac{1}{\ln(10)} \cdot \alpha d$$

This result shows that the optical density is proportional to the absorption coefficient.

Photoresponse

Heyningen and Brown (8) gave a derivation of the photo-response, conceived by K. Hecht (9), which is now briefly derived. When a single light pulse hits the crystal, electrons are released to produce a current driven by an electric field of $E = \frac{V}{d}$. The electrons released induce a charge on the electrodes of the measuring device (electrometer). The charge induced can be found if three assumptions are made. (i) The initial condition is that n_0 electrons are released at time $t = 0$. (ii) A uniform electric field exists throughout the crystal and is not reduced by the electron flow. (iii) There is a uniform density of electron traps. The mean trapping time of an electron is:

$$\tau_t = \frac{1}{N_t \sigma U}$$

where

N_t is the density of the traps

σ is the cross sectional area of the average trap

U is the thermal velocity of the electron

A displacement distance known as the Schubweg is defined as the displacement of an electron in the direction of the electric field before it is permanently trapped and is given by:

$$\omega = u E \tau_t$$

where

u is the electron mobility defined as the diffusion velocity divided by the electric field.

The number of free electrons at time t is given by:

$$n = n_0 e^{-t/\tau_t}$$

or since ω is proportional to τ_t :

$$n = n_0 e^{-x/\omega}$$

where

x is the distance the electron has traveled in time t in the direction of the applied electric field.

The amount of charge, q , induced on the electrodes for each electron which has a displacement x in the crystal is given by:

$$q = e \left(\frac{x}{d} \right)$$

The average displacement of all the electrons is $\bar{x} = \omega$. So the total charge induced on the electrodes is:

$$Q = e \left(\frac{\omega}{d} \right) \cdot n_0$$

where

d is the distance between the electrodes.

Now if we assume that the crystal has a uniform absorption constant and reflectivity we know the number of electrons present at time $t=0$ is given by:

$$n_0 = (1 - e^{-\alpha d}) \eta_a N_0 (1 - R)$$

where

N_0 is the number photons in the single light pulse

$(1 - R)$ is the transmittivity coefficient

$(1-e^{-\alpha d})$ is the fraction of photons absorbed (α is the absorption coefficient)

η_a is the number of electrons released per photon absorbed.

So the total amount of charge induced on the electrodes is:

$$Q = n_o e \left(\frac{\psi}{d} \right) = (1-e^{-\alpha d}) \eta_a N_o (1-R) e \left(\frac{\psi}{d} \right)$$

ω is usually normalized by the electric field to give:

$$\omega_o = \frac{\omega}{E}$$

So the induced charge on the electrodes becomes:

$$Q = \frac{\eta N_o e E \omega_o}{d}$$

where

$$\eta = (1-e^{-\alpha d}) \eta_a (1-R)$$

and is the quantum efficiency per incident photon i.e., η is the number of electrons released per incident photon. Differentiating Q with respect to time gives:

$$\frac{dQ}{dt} = \frac{\eta e E \omega_o}{d} \frac{dN_o}{dt} = I$$

where

I is the instantaneous photocurrent.

The equation can be rearranged to give the equation:

$$\eta \omega_o = \frac{I}{N_o} \left(\frac{d^2}{eV} \right)$$

where

η is the incident photon flux

e is the charge on an electron

V is the potential used to drive the carriers producing

the instantaneous current

d is the distance between the electrodes on which V
is maintained.

CHAPTER III

APPARATUS

Optical Density Measurements

This thesis is concerned mainly with photoconductivity and related optical absorption measurements made on corundum. The optical absorption measurements were made over the spectral range from 2 eV to 6 eV using a Cary 14 recording spectrometer. These measurements were made at a temperature of either 77 K or room temperature.

Photoconductivity Measurements

A block diagram of the apparatus for measuring the photo-response (ηW_0) is shown in Figure 2. The apparatus must be capable of measuring the photocurrent (I) and the incident photon flux (N) as a function of wavelength. The other parameters in the equation:

$$\eta \omega_0 = \frac{I d^2}{N_0 e V}$$

(See Chapter II) are constant with respect to wavelength.

The measurement of I is achieved by a vibrating reed electrometer (Cary 401) and the amplified signal is recorded on an X-t recorder (Omnigraphic Series - 2000). The parameter detects the small current produced in the sample by a

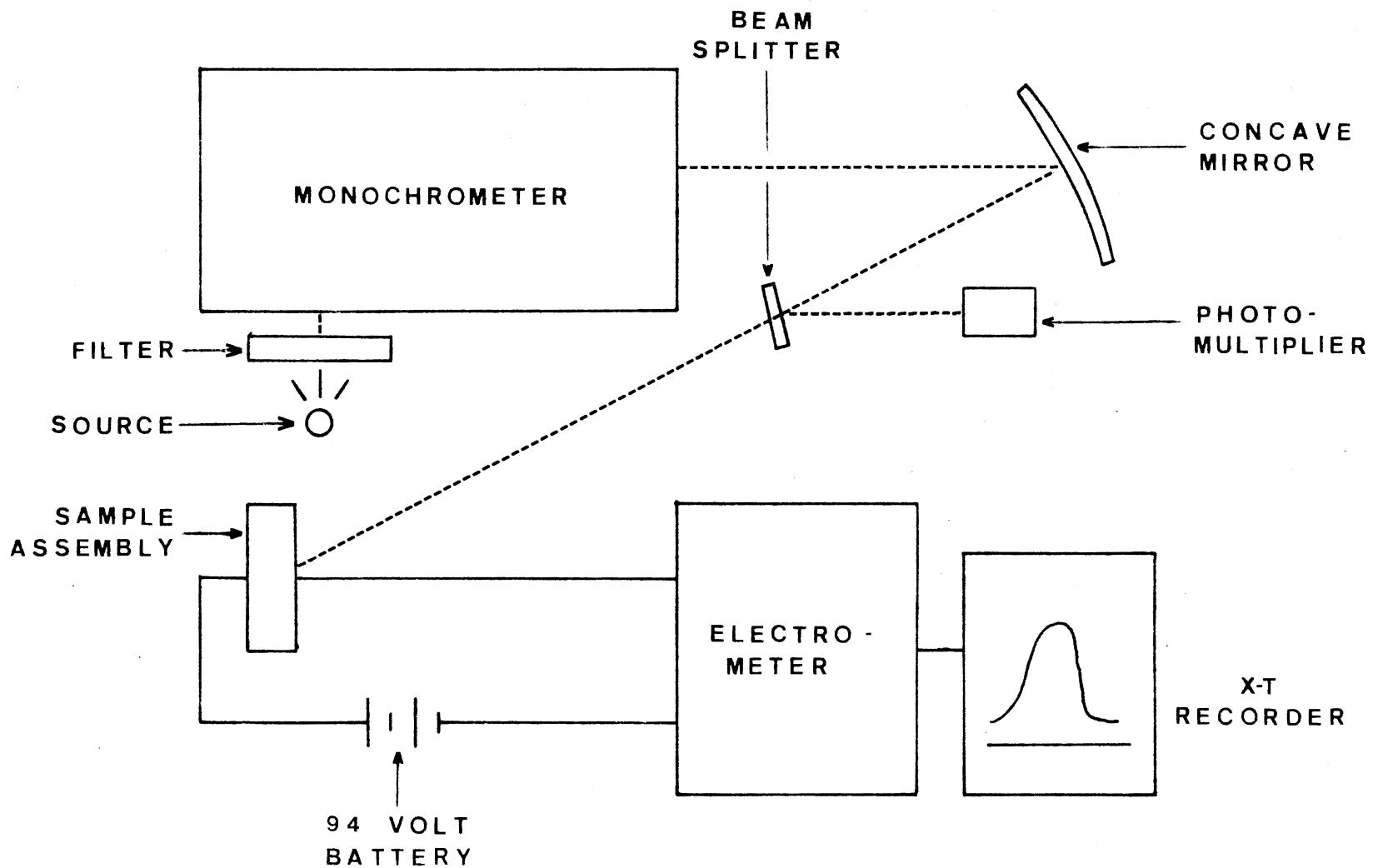


Figure 2. Block Diagram of Apparatus for Measuring Photoresponse.

polarizing potential of about 94 Volts, which produces an electric field of approximately 1000 Volt/cm across the sample. The polarity of the potential across the sample is controlled by a relay. Typical currents lie in the range of about 10^{-13} A to about 10^{-9} A. The light used to release electrons in the sample is produced by a 75 watt Xenon lamp with suitable filters to eliminate transmission of higher orders by the monochrometer. The light was dispersed by a McPherson 218, 1/3 meter monochrometer with a grating of 1200 lines permm blazed at 2000 Å. The light leaving the monochrometer impinges upon a concave mirror where it is focused onto the sample. Part of the incident beam is split off and sent to a photomultiplier tube which is used to monitor the beam intensity. The intensity of the light flux is typically about 10^{11} to 10^{13} photons per second from wavelengths of about 190 to 400 nm.

A schematic diagram of the sample assembly is shown in Figure 3. The sample was isolated from the electrodes by two thin slabs of sapphire. The front electrode is made of a fine phosphor-bronze wire gauze to permit light to fall onto the sample. The rear electrode is thin copper foil. There was some concern whether the photoconduction of the sample would be affected by the nature of the electrode blocking material since the sample and blocks were of the same material. A block of SrF_2 was made to investigate this possibility. There was no detectable difference using sapphire or SrF_2 for the blocking material. The light incident on the sample

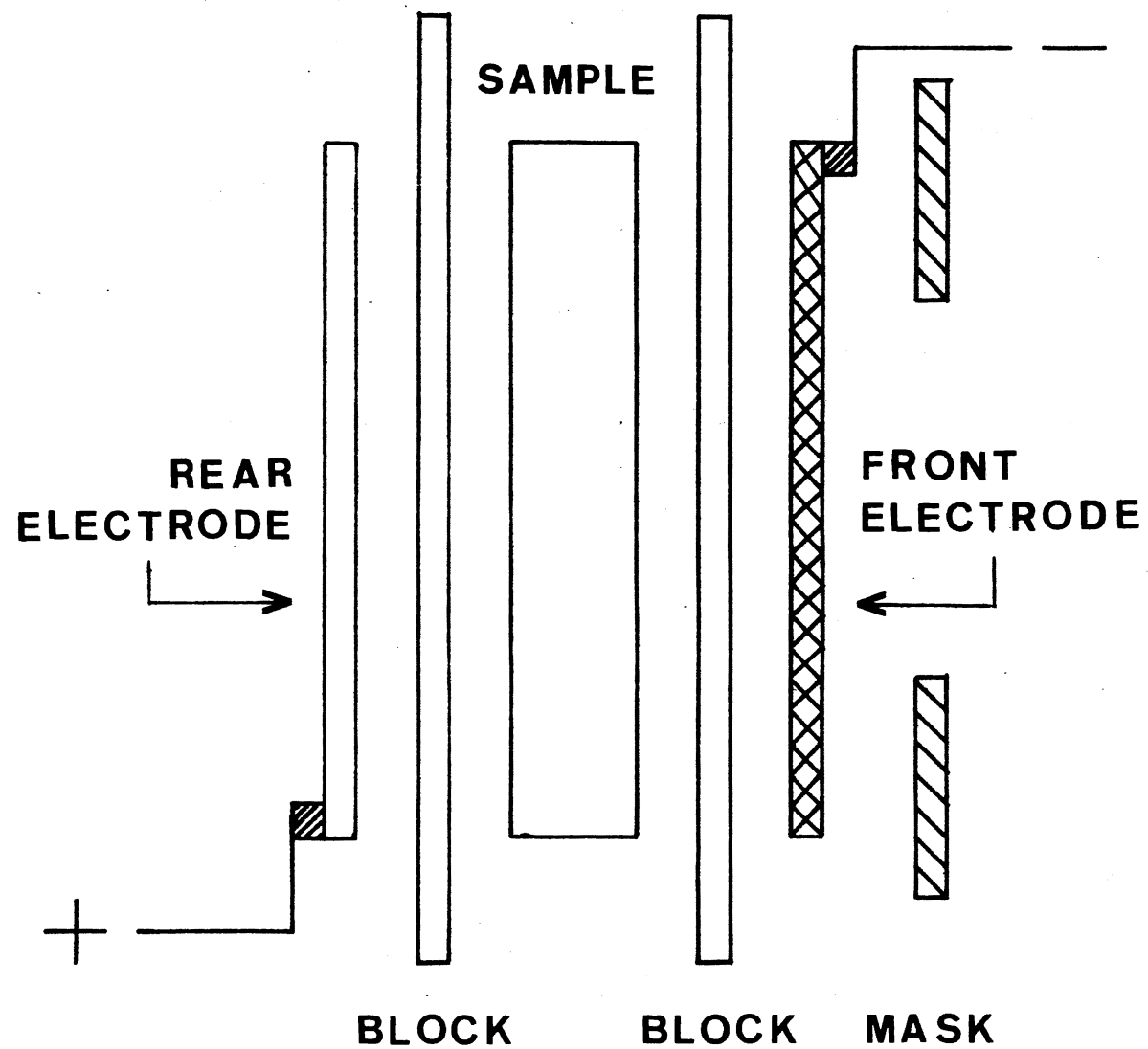


Figure 3. Schematic Diagram of the Sample Assembly.

was restricted to a 7.5 mm by 3 mm area by a black paper mask.

The sample was located inside a cryostat to permit temperature variation from liquid helium temperature to room temperature. The temperature was monitored by a copper-constantan thermocouple referenced at 0°C. The potential difference across the thermocouple was measured by a Leeds and Northrup 8691-2 millivolt potentiometer. The windows of the cryostat are of fused quartz, which is transparent over the wavelength range used.

Measurement of the incident light intensity was made as follows. A Molelectron pyroelectric radiometer was set in place of the sample to find the amount of energy falling on the sample for a given wavelength (a constant band-width of 4 nm was used). The radiometer has a calibration traceable to the National Bureau of Standards. The power, P , from the Xenon lamp is given by:

$$P = N_o E = N_o h \nu = \frac{N_o h c}{\lambda}$$

where

E is the energy of each photon

h is Planck's constant

ν is the frequency of the light

c is the velocity of light.

The equation can be solved for N_o to give:

$$N_o = \frac{P \lambda}{h c}$$

N_o is plotted against λ in Figure 4. Because of the relatively

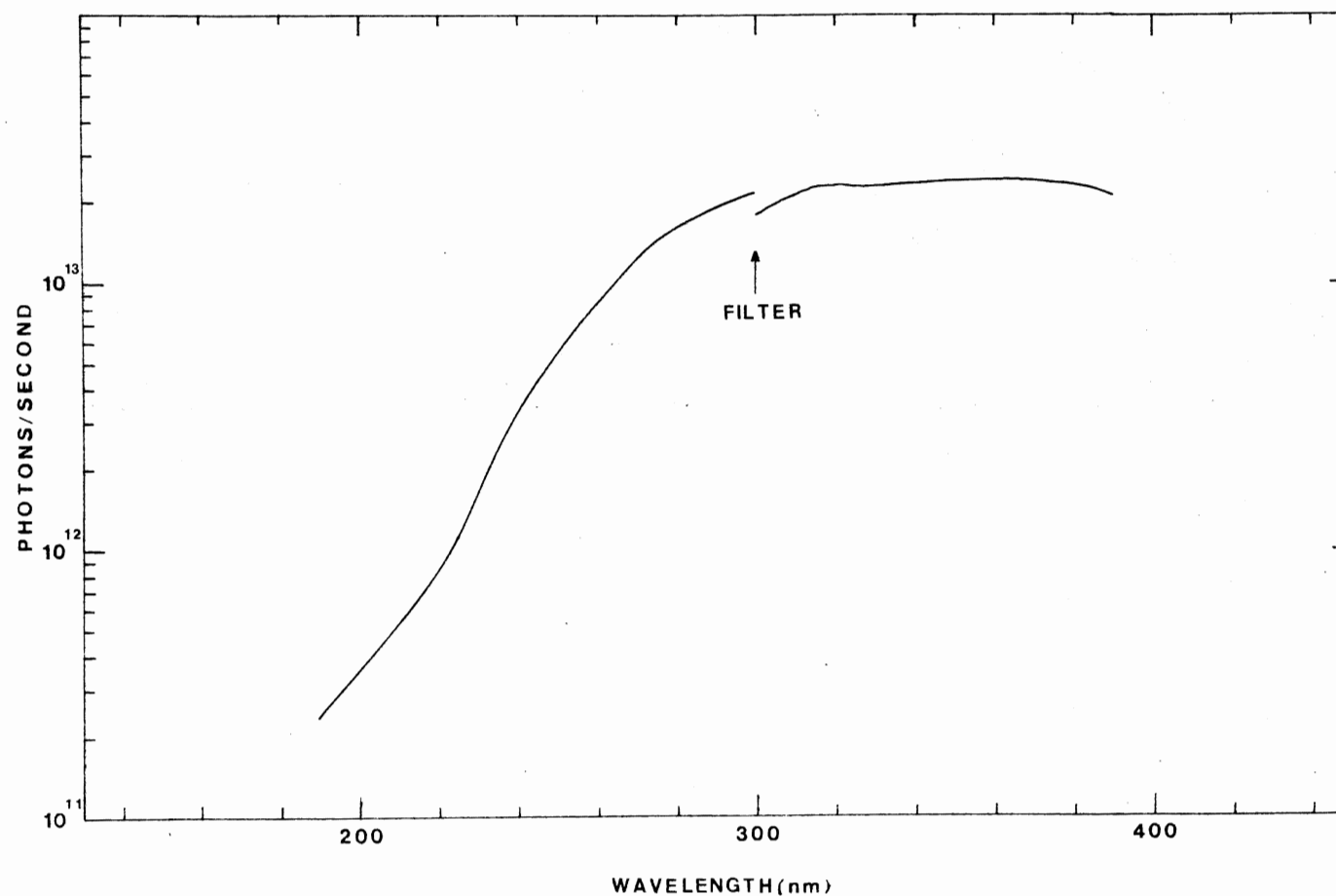


Figure 4. Photon Flux as a Function of Wavelength. Measurements for incident light of wavelengths less than or equal to 300 nm were made with a photomultiplier. A radiometer was used for wavelengths greater than 300 nm.

low output of the lamp below 300 nm the first part of the curve up to 300 nm was also measured using a photomultiplier tube (McPherson Model 650), which gives an output proportional to the number of photons incident on a sodium salicylate phosphor. The photomultiplier was calibrated in a separate experiment with the radiometer. The voltage used on the photomultiplier was 400 volts. The monitoring photomultiplier tube is an EMI 6256S and gave a current of .75 μ A at 290 nm at the time the power data was taken. The voltage for it was also 400 volts. The curve that was plotted can now be used to find the number of photons at a particular wavelength by taking the ratio of the monitoring photomultiplier current at 290 nm during a particular experiments to .75 μ A, and multiplying the ratio times the number of photons per second shown on the graph. The ratio varies slightly from experiment to experiment because of the characteristics of the lamp and power supply. The front blocked electrode and cryostat windows absorbed some light. The percentage of transmission due to these components is 37% and independent of wavelength over the range of about 190 nm to 560 nm. The intensity of light at the sample position was observed with and without the electrode and windows for various wavelengths. The ratio of the intensity gave the percentage of transmission.

Luminescence Measurements

A block diagram of the apparatus used to measure luminescence spectra is given in Figure 5. The apparatus must be capable of permitting monochromatic light to fall on the sample, and of detecting the emitted light.

The sample was located inside a cryostat which enabled

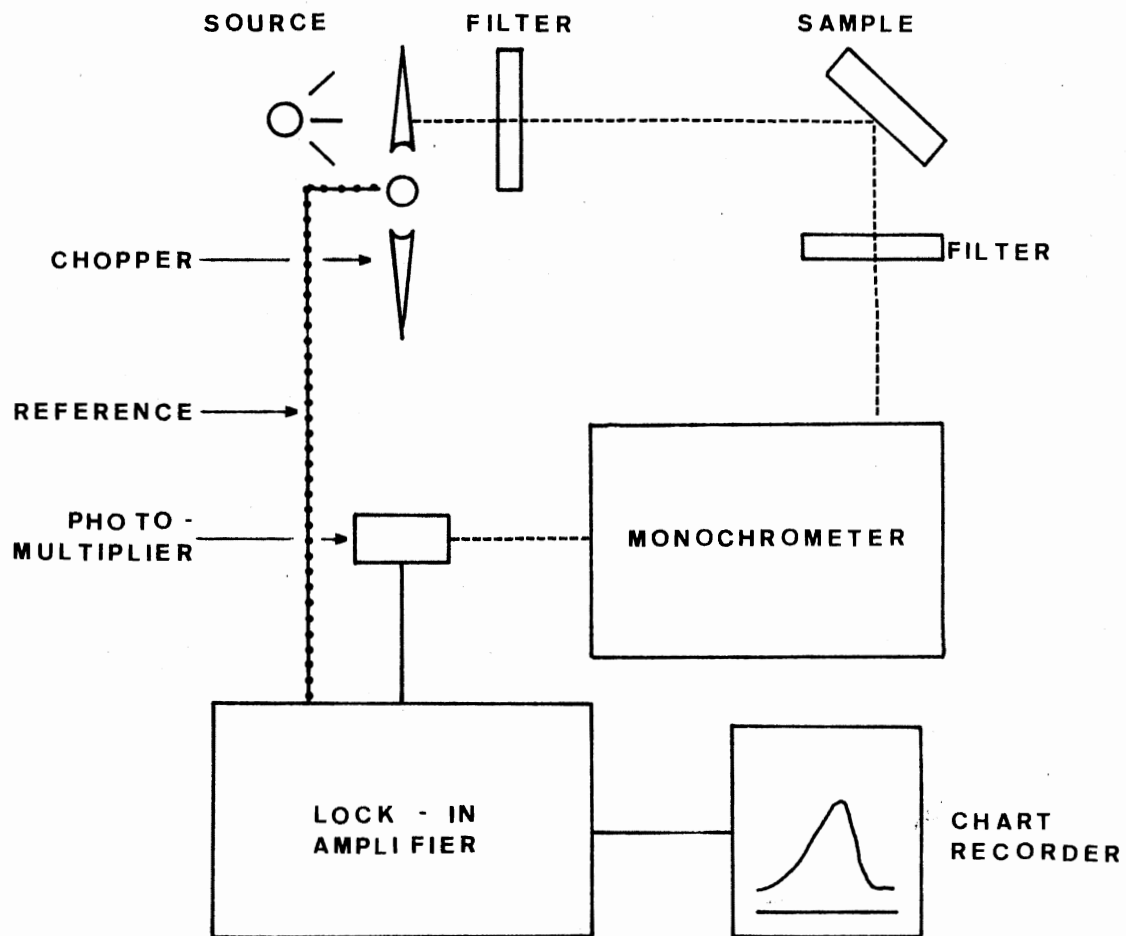


Figure 5. Block Diagram of the Apparatus for Measuring Luminescence.

its temperature to be varied between 4.2 K and room temperature. The windows of the cryostat are fused quartz, which permitted light from a deuterium lamp to fall on the sample. The incident light was made monochromatic by interference filters. The filters used, have transmission peaks at 2014\AA and 2522\AA . The incident light was chopped by a mechanical chopper to permit detection of the light emitted by the sample with a PAR model 128A lock-in amplifier. The emitted light was dispersed by the McPherson monochromator with a grating blazed at 2000\AA . Optical filters were placed between the sample and the monochromator whenever necessary to reduce stray light and higher order effects. Detection of the emitted light was made with a thermoelectrically cooled RCA C31034 photomultiplier tube. The signal was amplified by the lock-in amplifier and recorded on a Model SR-205 chart recorder from Schlumberger.

The apparatus for the excitation spectra is identical to that of the emission spectra except a scanning Jarrell-Ash monochromator is used to disperse the incident light instead of the interference filters. To define the incident light energy, the incident wavelengths are scanned instead of the emitted light as in the emission spectra.

Irradiations

Samples were gamma irradiated at room temperature with a Gamma-Cell - 200 tank, using Co^{60} as a source. The strength of the source is about 4×10^4 R/hr. The irradiation time was one week.

The electron irradiations were performed at 77 K using a 1.5 MeV Van de Graaff accelerator. The low temperature was maintained in an optical cryostat containing an aluminum window through which incident electrons could easily pass. The beam current incident on the sample was found by fashioning a copper foil in the same shape as the crystal, and determining how much total current must be produced by the Van de Graaff in order to get 1 μ A to fall on the samples after passing through two aluminum windows and about 5 cm of air. The optical absorption changes introduced into the sample by the irradiation were monitored on the Cary to insure that damage had been sustained by the sample.

CHAPTER IV

RESULTS AND DISCUSSION

Nominally Pure Sapphire

Non-Irradiated Sapphire

Undoped samples of sapphire were obtained from several different sources. Samples of dimensions 10 mm x 5 mm x 1.5 mm were obtained from Linde. These crystals were the cleanest crystals from both optical absorption and photoconductivity measurements. Other undoped samples came from Crystal Systems, Adolf Meller, and International Sapphire (Insaco) companies. The thicknesses of these crystals are 1 mm, 1.5 mm, and 1.5 mm respectively. The original source of the crystals received from Insaco is unknown. The crystals were polished to an optical finish (approximately 6 microns).

The photoresponse for several of the undoped and "as received" samples at room temperature are shown in Figure 6. The photoresponse is shown in curves a, b, and c for crystals from Adolf Meller, Insaco, and Crystal Systems companies respectively. The Linde sample had no measurable photoresponse. All but the Linde sample have peak positions at about 5.9 eV.

Optical absorption spectra for the undoped and "as received" samples are shown in Figure 7. Curves a, b, c, and d are optical absorption spectra for crystals from Linde, Crystal

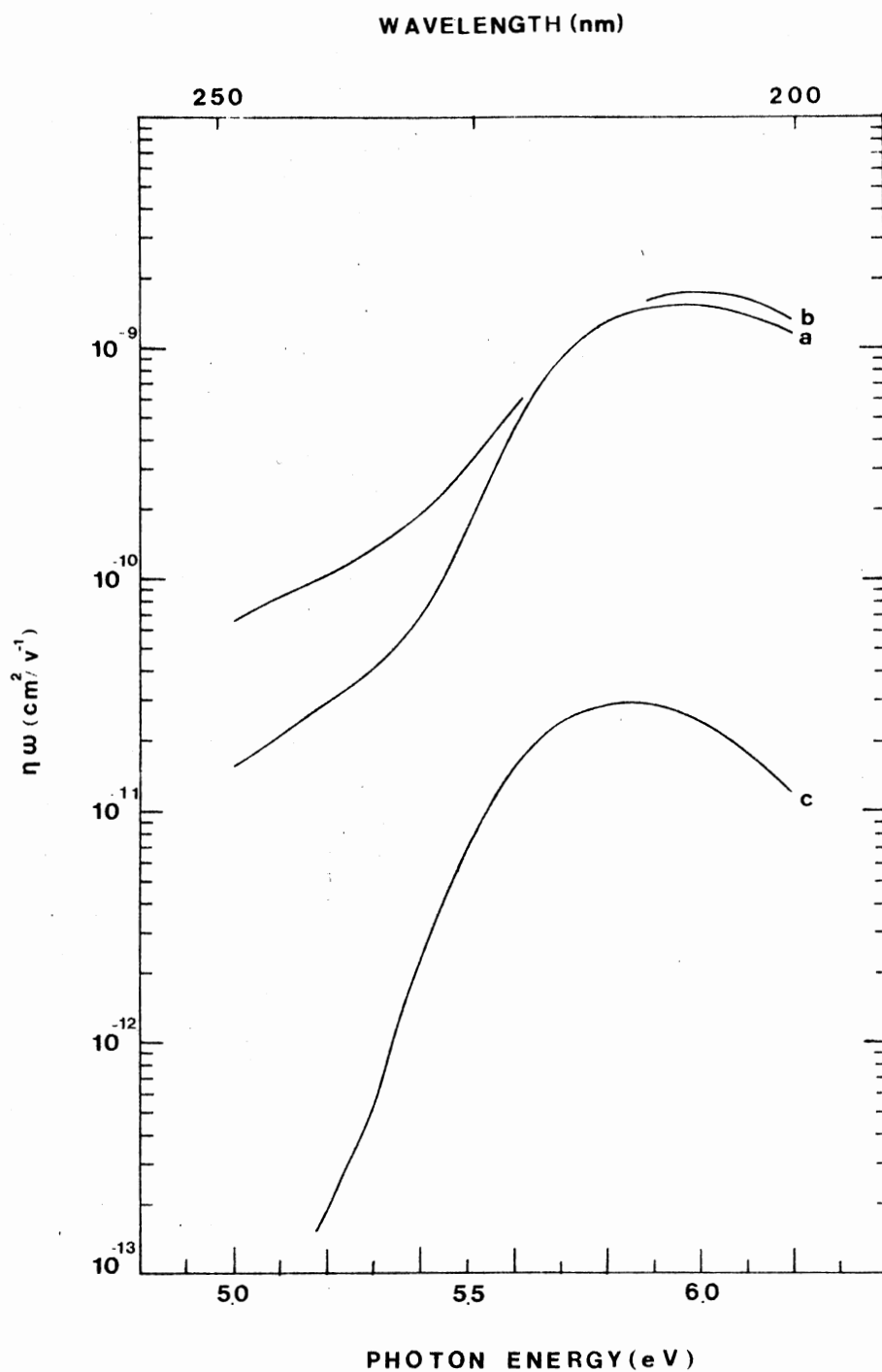


Figure 6. Spectral Dependence of the Photoresponse at Room Temperature for "As Received" Crystals of Al_2O_3 : Adolf Meller Sample, Curve a; Insaco Sample, Curve b; and Crystal Systems Sample, Curve c.

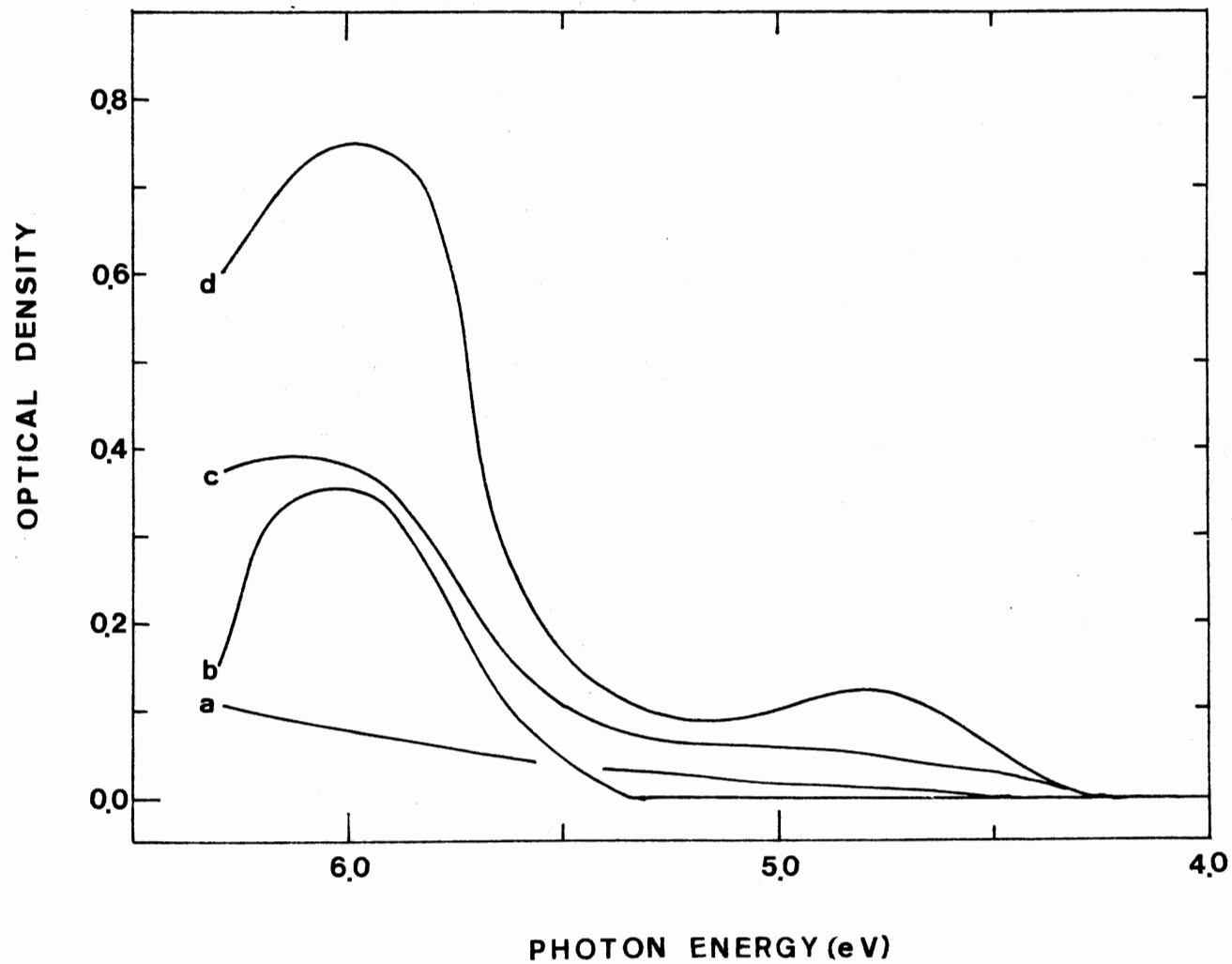


Figure 7. Optical Absorption Spectra at Room Temperature of "As Received" Samples of Al_2O_3 : Linde Sample, Curve a; Crystal Systems, Curve b; Adolf Meller, Curve c; Insaco, Curve d.

Systems, Adolf Meller, and Insaco companies respectively. It can be seen that the optical absorption bands peak in the region of 5.9 eV similar to the photoresponse spectra. In addition the Insaco sample has an optical absorption band located at 4.8 eV.

Electron-Irradiated Sapphire

Electron irradiation of a Linde crystal gave the photoresponse spectrum shown in Figure 8 at room temperature (curve a) and at 77 K (curve b). The peaks at room temperature lie at about 3.8 eV and 4.95 eV.

The photoresponse at 77 K shown as curve b in Figure 8, the electron-irradiated sapphire peaks located at about 4.1 eV, 5.3 eV, and 5.9 eV. The 5.9 eV band corresponds to the 5.9 eV band in the non-irradiated samples in Figure 6. For a matter of completeness the optical absorption spectrum of the electron irradiated sample is shown on Figure 9 at 77 K. Peaks occur at 4.9 eV and 5.6 eV.

γ -Irradiated Sapphire

The photoresponse at room temperature of a γ -irradiated Linde sample is shown as curve a in Figure 10. A broad photoconduction band appears at about 5.8 eV. This is very close to the 5.9 eV band of the non-irradiated samples. The signal at room temperature is about three orders of magnitude larger than the electron-irradiated samples, and may mask underlying structure similar to that of the electron-irradiated sample.

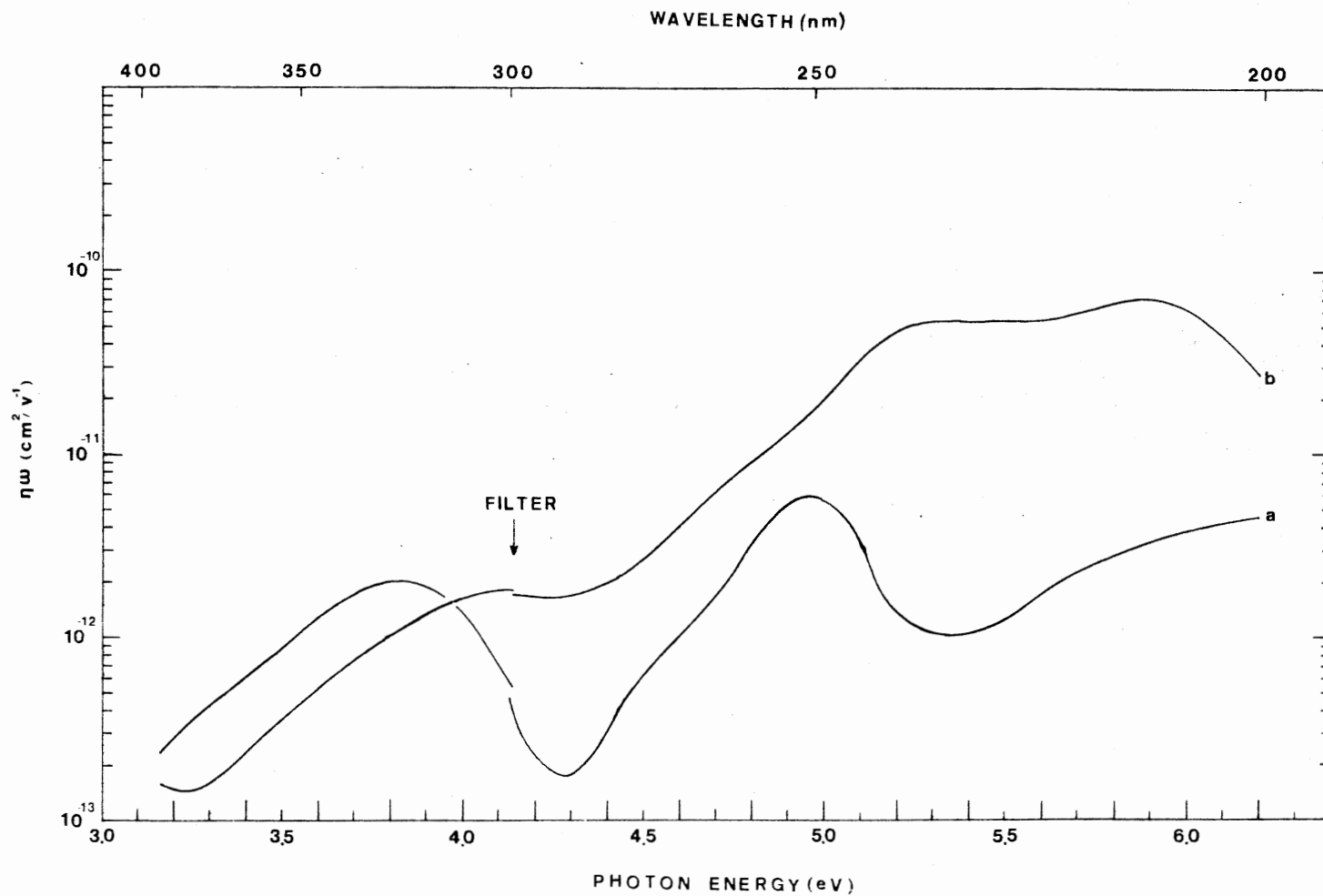


Figure 8. Spectral Dependence of the Photoresponse for Electron-Irradiated Al_2O_3 . The sample was irradiated at 77 K with 1.5 mev electrons to a dose of about 4.5×10^{16} electrons/ cm^2 . Measurements were made at room temperature (curve a) and 77 K (curve b).

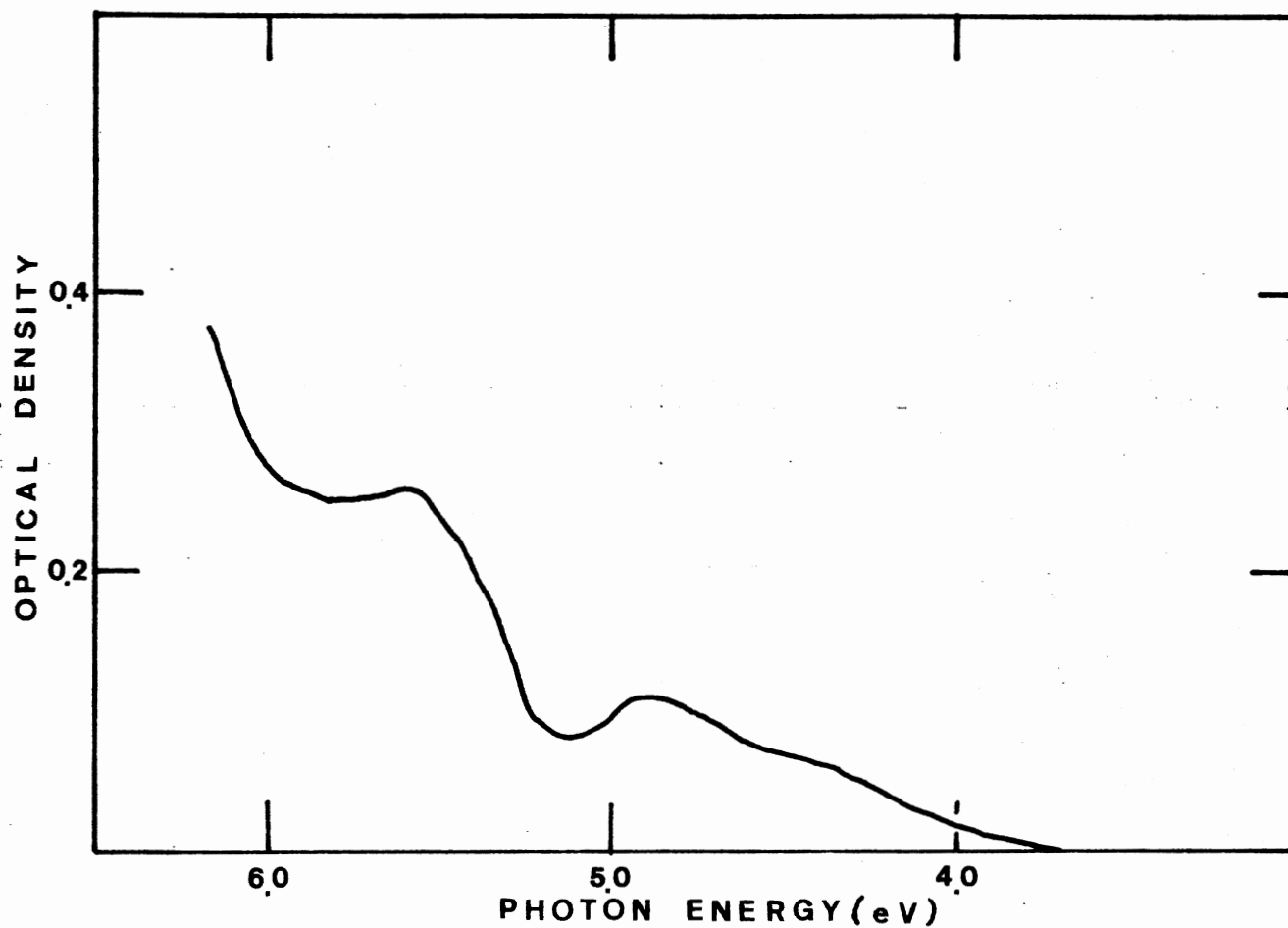


Figure 9. Optical Absorption Spectrum at 77 K of Electron-Irradiated Al_2O_3 . The sample was irradiated at 77 K with 1.5 mev electrons to a dose of about 4.5×10^{16} electrons/cm².

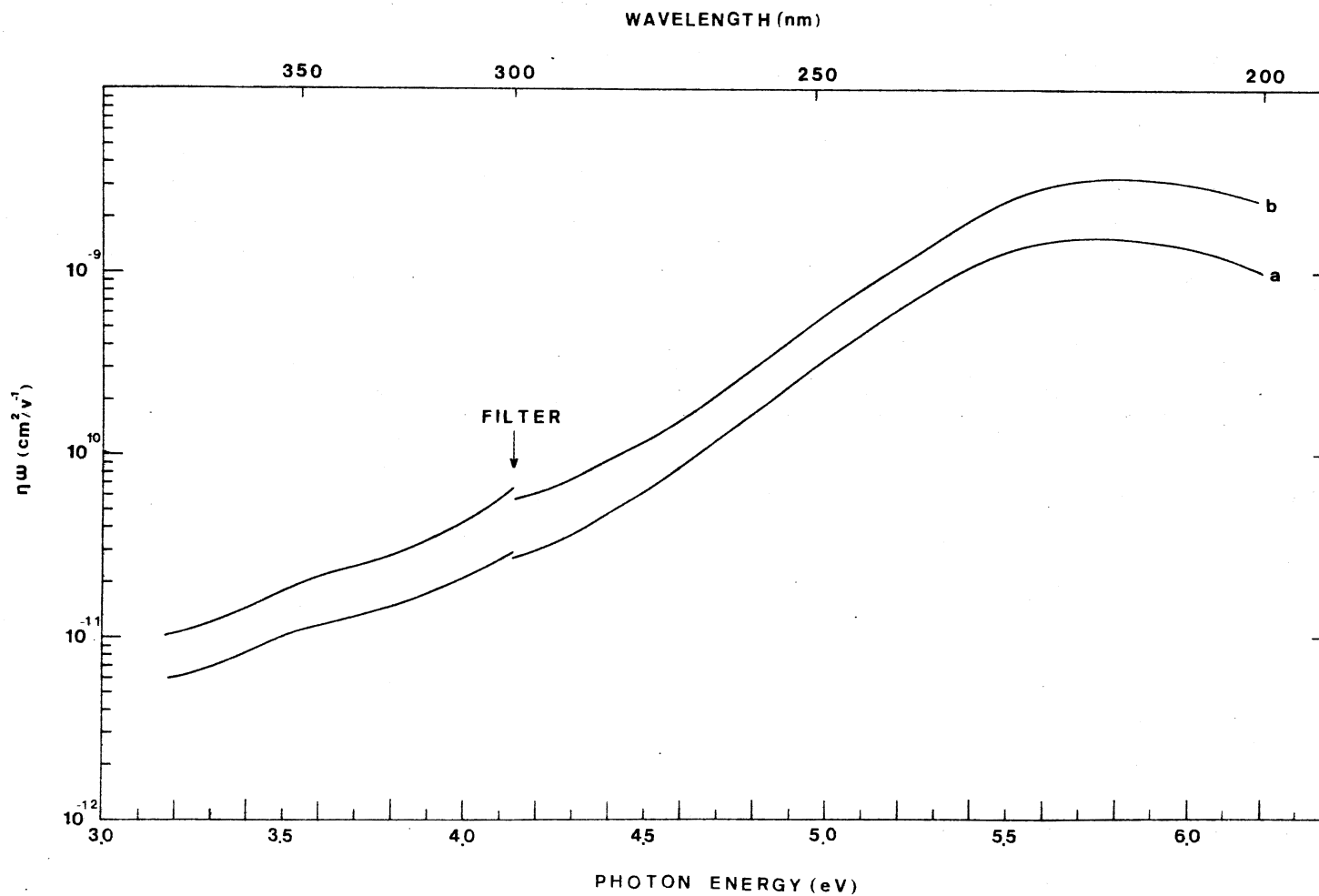


Figure 10. Spectral Dependence of the Photoresponse at Room Temperature of a γ -Irradiated Sample of Al_2O_3 (Curve a) and the Same Sample after a 15 minute Bleach at Room Temperature with 5.3 eV Light (Curve b).

The photoresponse became immeasurably small at a temperature somewhat below room temperature.

Bleaching the sample with 5.3 eV light, which is the same wavelength as a charge transfer band in ruby, for 15 minutes produces an interesting effect, which is that the photoresponse over the spectral range from 3 eV to 6.5 eV was increased as shown in Figure 10. The photoresponse after bleaching is shown in Figure 10 as curve b. A similar effect happens in γ -irradiated ruby which will be discussed below.

Optical absorption spectra at room temperature of the non-irradiated Linde sample (curve a) and the γ -irradiated Linde sample (curve b) is shown in Figure 11. The optical density of the irradiated sample diverges from that of the non-irradiated sample at around 5.3 eV and continues to diverge until about 6.4 eV which represents the limit of our measurements.

Discussion of Nominally Pure Sapphire

It is tempting to assign the photoconduction bands at about 5.9 eV to the iron group impurities, which have optical absorption peaks in the region about 5.9 eV (2). The results are inconclusive at this point, because as is shown below even though the bands are in the correct places, no correlation has yet been found between the photoresponse and deliberate doping of samples with iron group ions. The apparent lack of correlation could be due to strong trapping which could be caused by the doping process and which would decrease the effective range of the carriers, and thus make the photoresponse too small to be measured.

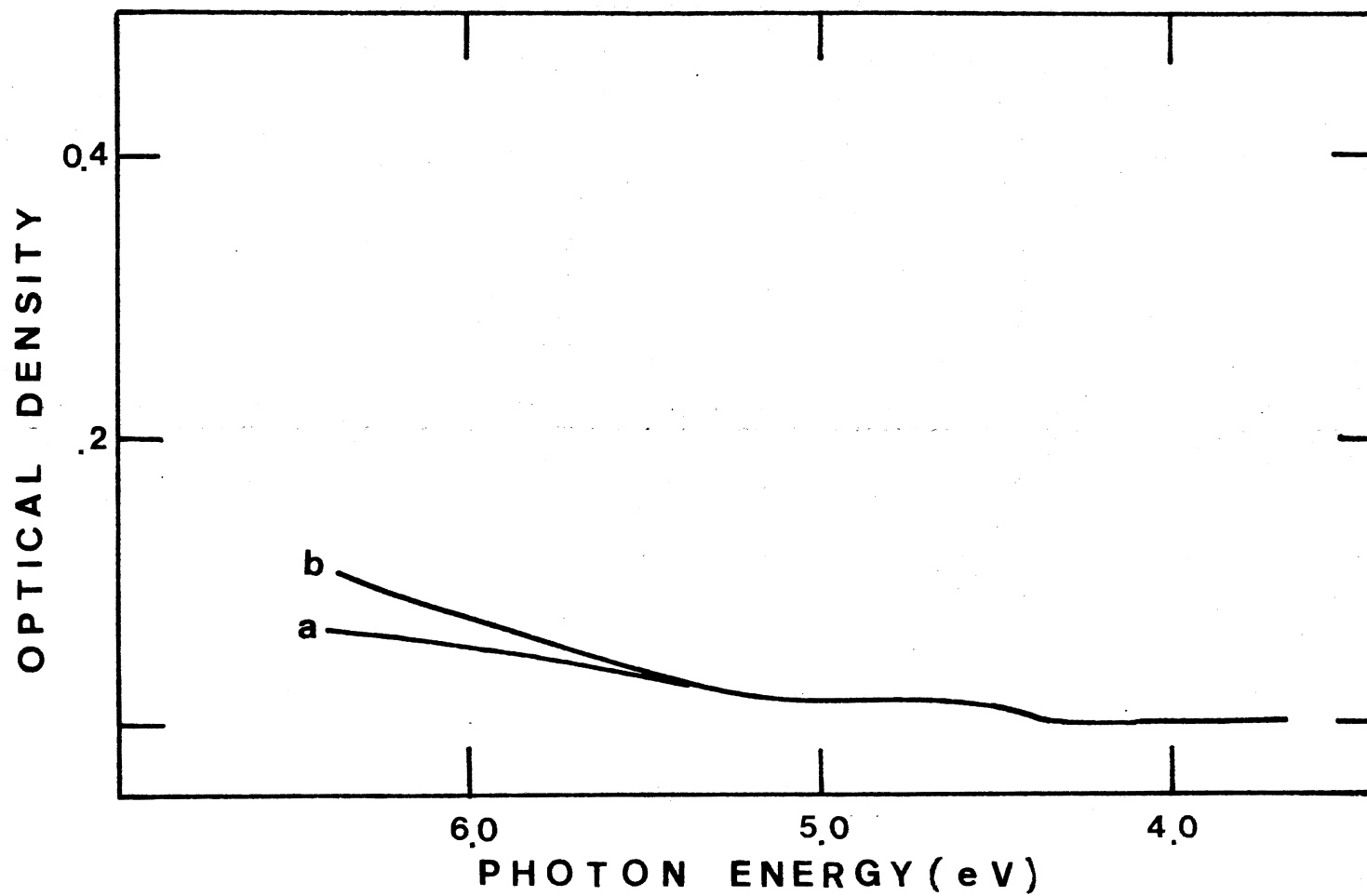


Figure 11. Optical Absorption Spectra at Room Temperature of Al₂O₃:
Non-irradiated sample, curve a; γ -irradiated sample
(curve b).

Nominally Pure Sapphire

General Description of Samples

Samples of sapphire were obtained with two different dopants. The dopants are Cr^{3+} and V^{3+} . Samples of $\text{Al}_2\text{O}_3:\text{Cr}^{3+}$ (ruby) were obtained from the Linde company. These samples are 1.5 mm thick and contain nominally 300 PPM of Cr^{3+} . The V^{3+} doped samples were obtained from Crystal Optics Research. The thicknesses of these samples are 1.5 mm and .5 mm. The V^{3+} doped samples contain nominally 100 PPM of V^{3+} ions.

V^{3+} Doped Sapphire

The V^{3+} doped samples gave no measurable photoresponse, indicating that V^{3+} ions were probably not responsible for the 5.9 eV band of the undoped samples.

The optical density for $\text{Al}_2\text{O}_3:\text{V}^{3+}$ is shown in Figure 12. Peaks can be seen to occur at 5.71 eV and 3.09 eV. The lack of correspondence to the 5.9 eV optical absorption band of the undoped samples again indicate that the 5.9 eV photoconductivity bands aren't produced by V^{3+} ions.

Non-Irradiated Ruby

The photoresponse in non-irradiated ruby is shown in Figure 13, curve a. The photoresponse shows a gradual increase from about 4.0 eV to about 4.95 eV, and then a sharper increase to about 5.9 eV where it begins to level off until around 6.2 eV. The peak is at about the right wavelength to produce the 5.9 eV band in the undoped samples until the ruby

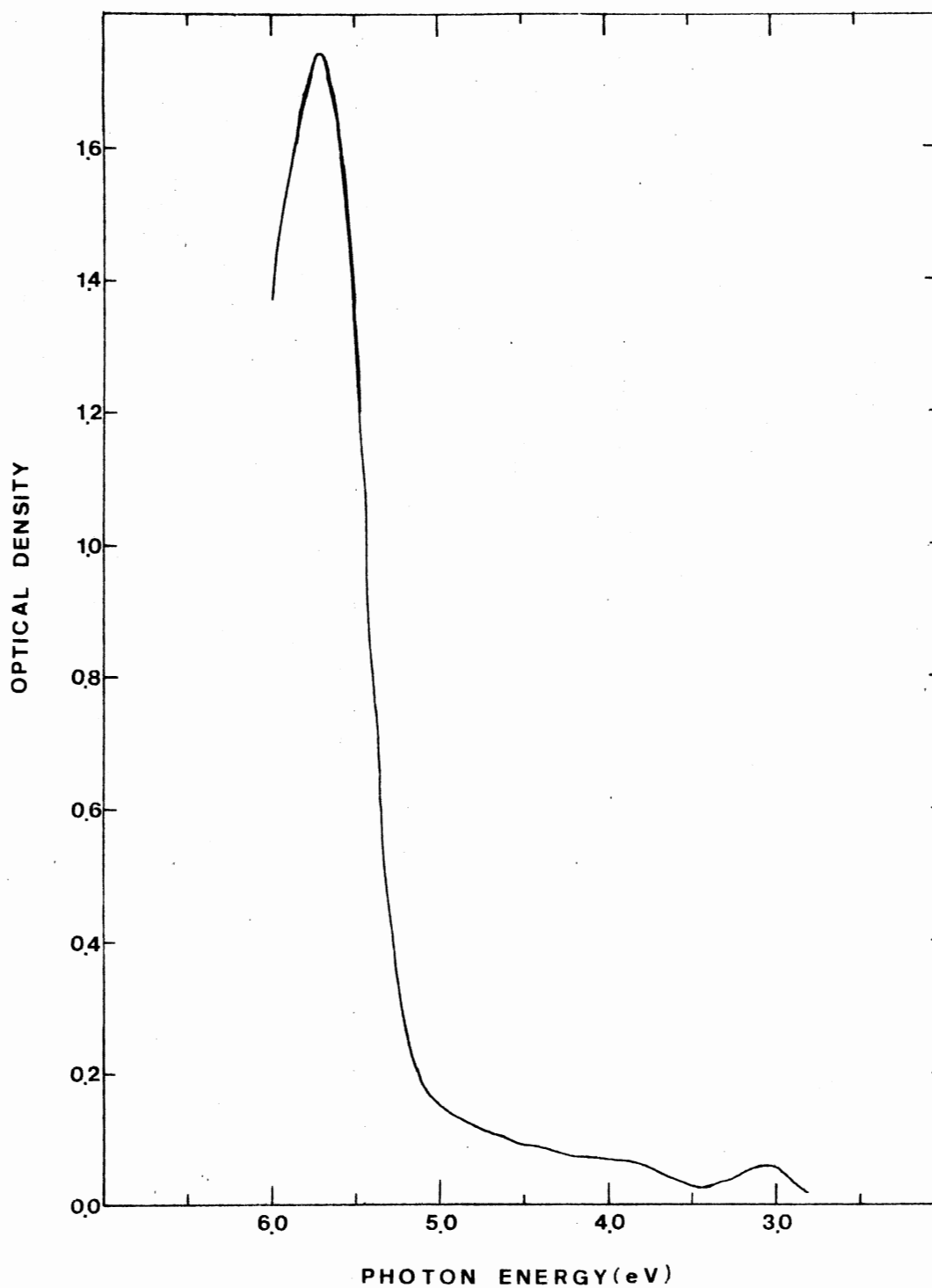


Figure 12. Optical Absorption at Room Temperature for "As Received" Sample of Al₂O₃ Doped with 100 ppm of V³⁺.

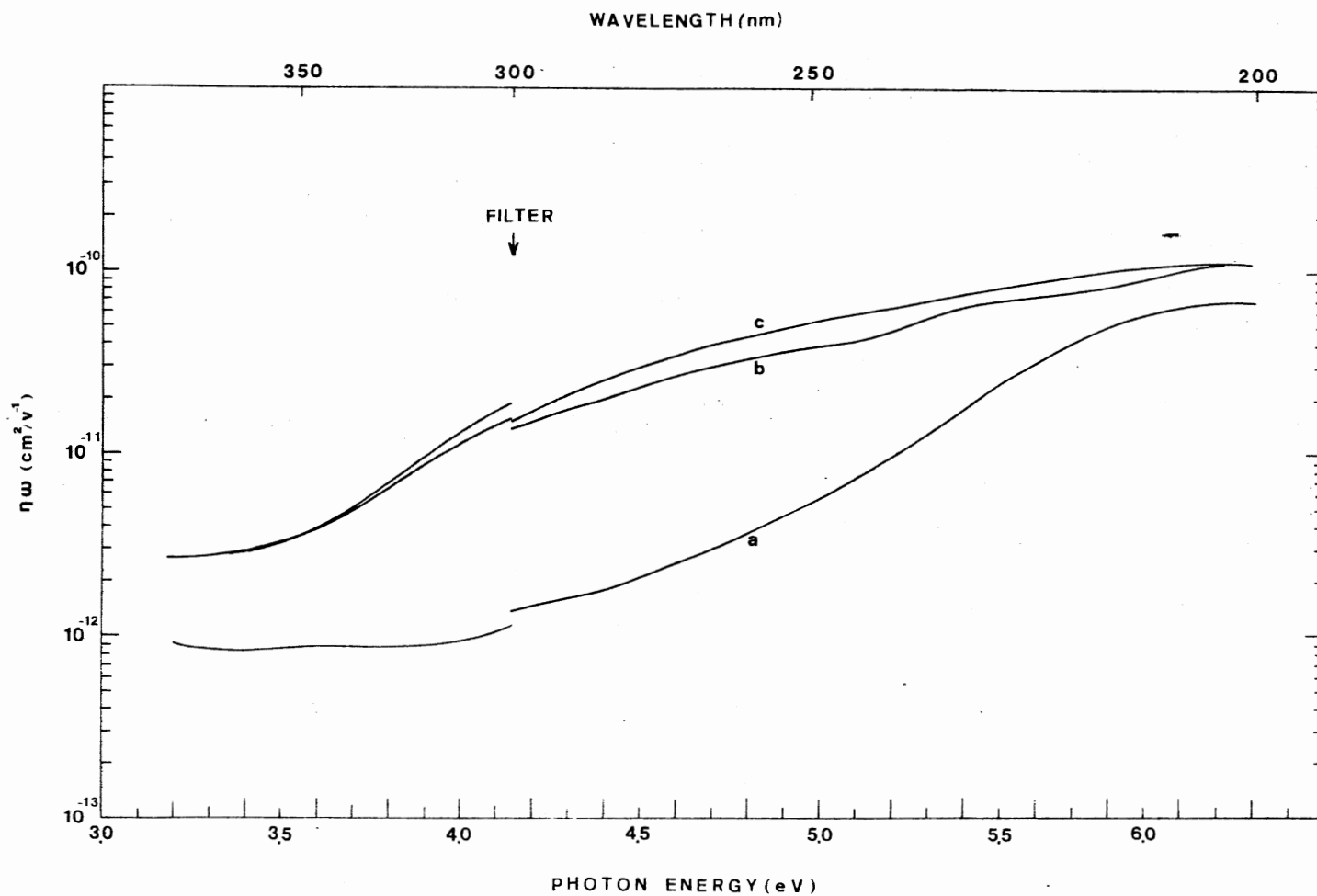


Figure 13. Spectral Dependence of the Photoresponse at Room Temperature of Ruby: Non-Irradiated Sample, Curve a; γ -Irradiated Ruby, Curve b; the γ -Irradiated Sample after Bleaching at Room Temperature for 15 minutes with 4.4 eV Light, Curve c.

samples are irradiated as will be shown below.

The optical absorption spectrum of non-irradiated ruby at room temperature is shown as curve a in Figure 14. Peaks due to internal transitions of Cr^{3+} are located at 2.2 eV and 3.05 eV. There is also a hint of a peak at 5 eV.

γ -Irradiated Ruby

The photoresponse of non-irradiated ruby is shown as curve a in Figure 13, and the photoresponse of γ -irradiated ruby is shown as curve b in Figure 13. It can be seen that after γ -irradiation the photoresponse increased generally over the whole range of energies from 3.2 eV to 6.2 eV. A difference curve between a and b of Figure 13 reveals that a band grew in around 5.4 eV. This band is shown as curve b on Figure 18. Optical bleaching for 15 minutes at 4.4 eV using a xenon lamp gives rise to a slight increase of the photoresponse over the range of 3.7 eV to 6.1 eV. The photoresponse after the optical bleach is shown in Figure 13, curve c.

Curve a of Figure 14 shows the optical absorption spectrum of non-irradiated ruby at room temperature. Curve b of Figure 14 shows the optical absorption spectrum at room temperature of ruby after γ -irradiation. After γ -irradiation a large optical density is seen beginning at 3.5 eV and steadily increasing as the incident photon's energy increased. There is a shoulder on the increasing curve at about 4.1 eV. The 4.1 eV shoulder is possibly due to charge transfer trans-

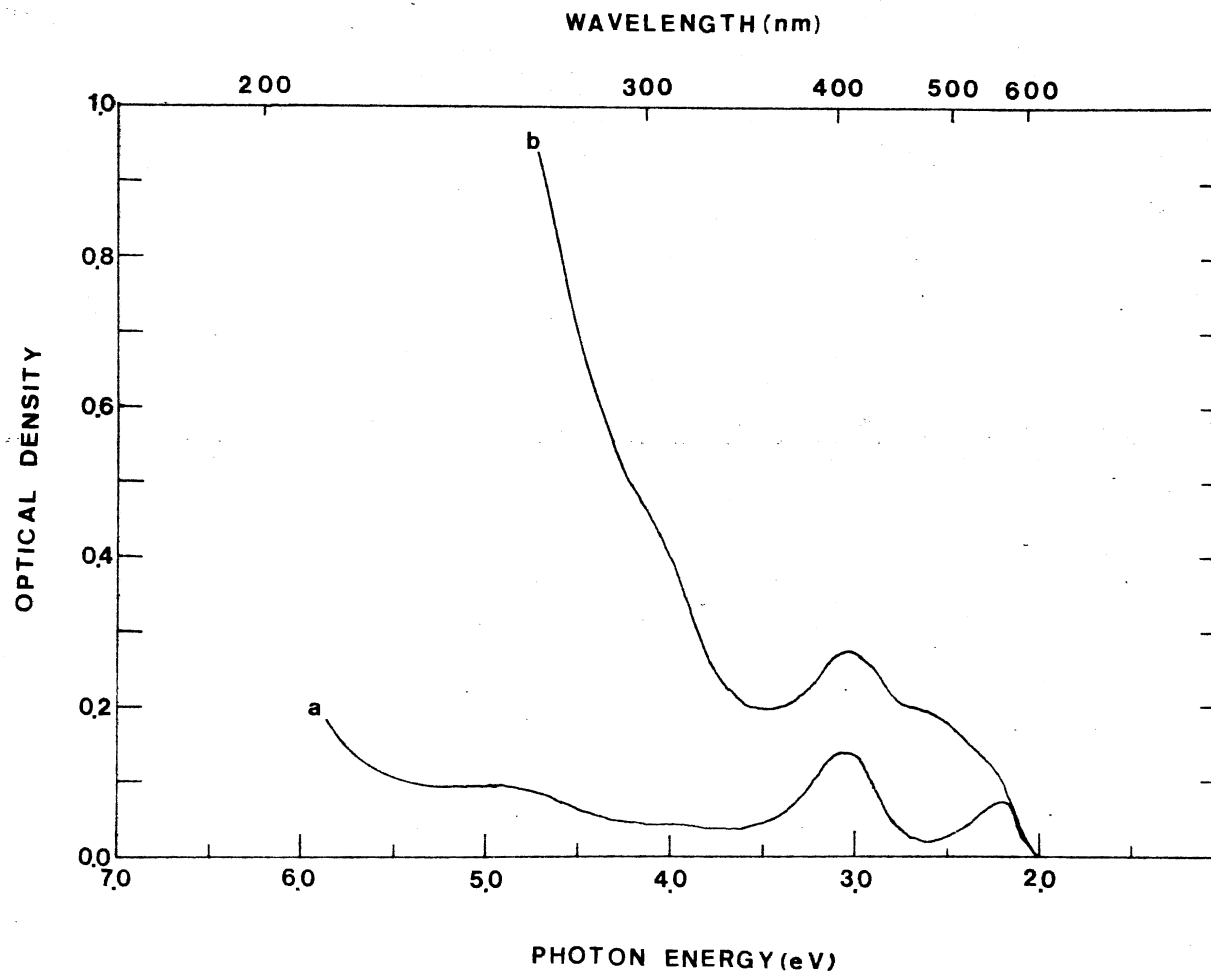


Figure 14. Optical Absorption Spectra at Room Temperature of Ruby: Non-Irradiated Sample, Curve a; γ -Irradiated Sample, Curve b.

itions of chromium with a valence different than 3^+ . The small peak at 2.5 eV has not yet been identified. Turner and Crawford (4) have concluded that the band at 5.4 eV is due to Cr^{2+} caused by a Cr^{3+} ion capturing an electron. Klaffley and Rose (5) have suggested that Cr^{4+} ions have been observed by esr measurements in electron irradiated ruby. McClure (6) suggests that both Cr^{2+} and Cr^{1+} are stable in sapphire, so that the causes of the bands at 4.1 eV and 5.4 eV depend on whether the dominant traps are holes or electrons. This is not presently known. Optical bleaching at room temperature with 4.4 eV light using a xenon lamp for 2 hours produced a decrease in the optical absorption spectrum of γ -irradiated ruby over the range of energies from 2.18 eV to 6.2 eV.

Since the photoresponse increased upon bleaching the γ -irradiated sample with 4.4 eV light and the number of photo-centers did not increase as shown by the decrease of the optical absorption spectrum which is shown in Figure 15, the crystal was bleached with 4.4 eV light, we concluded that the increase in photoresponse with optical bleaching must be due to an increase in the range of the charge carriers. The increase in range was apparently produced by filling of available traps in the crystal.

As shown in Figure 13, the photoresponse grows as the sample is bleached with 4.4 eV light. The time dependence of this growth is shown in Figure 16. The photocurrent appears to asymptotically approach a maximum value. However,

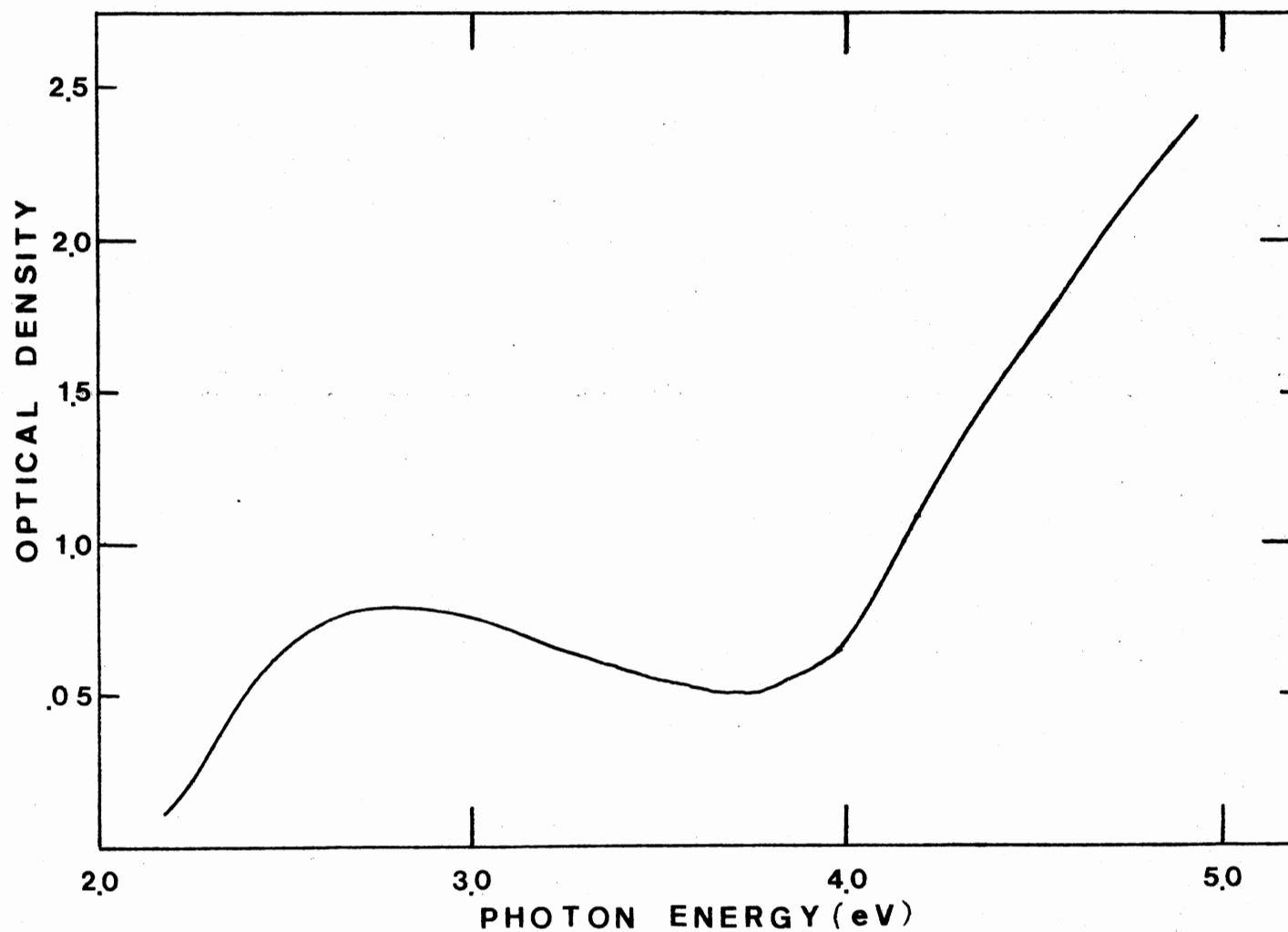


Figure 15. Difference Curve Between Optical Density Absorption Spectra of γ -Irradiated Ruby at Room Temperature Before and After Bleaching for one hour with 4.4 eV Light.

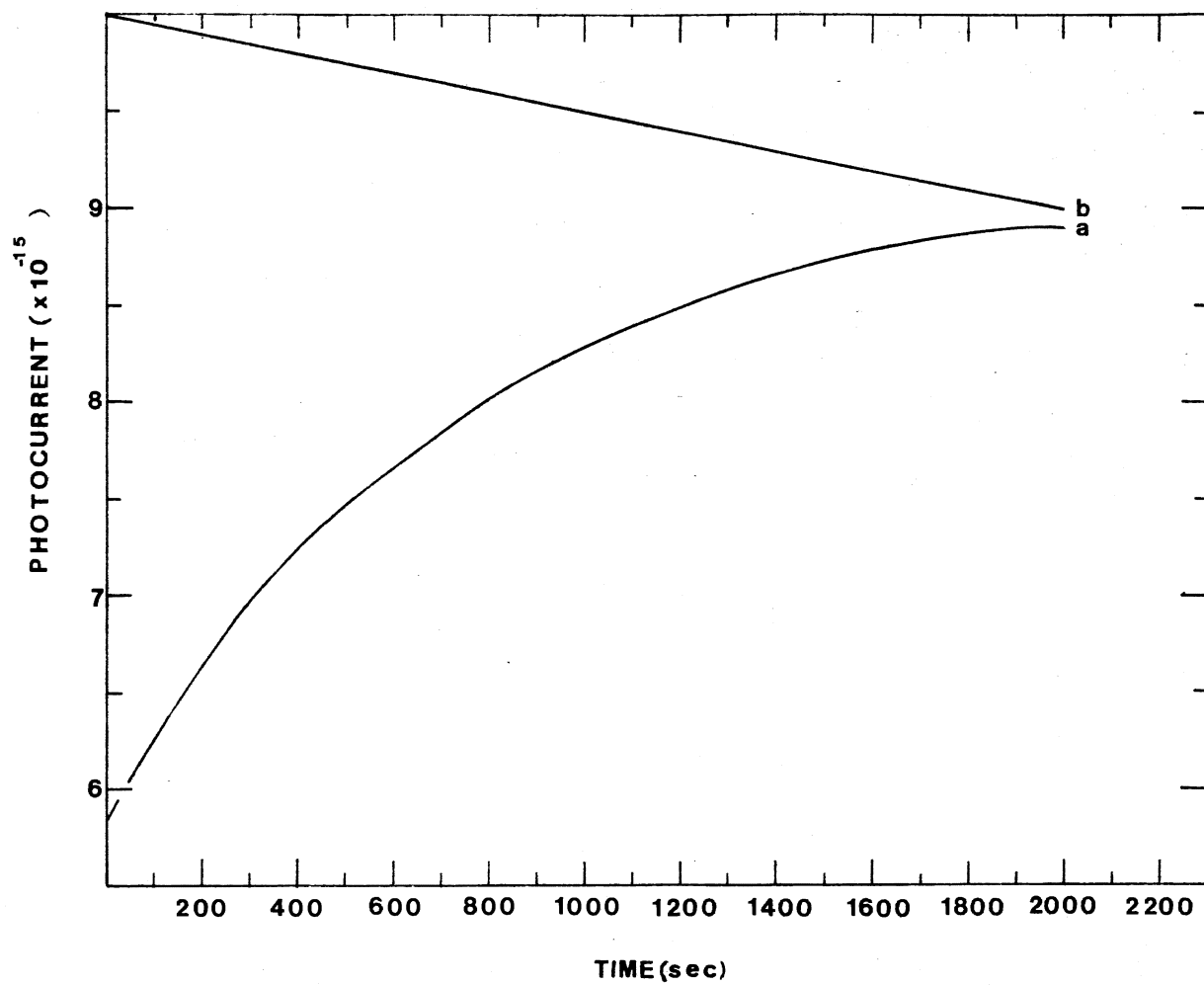


Figure 16. Photocurrent at 4.4 eV at Room Temperature as a Function of Time: Decay Curve, Curve a; Growth Curve Obtained by Bleaching with 4.4 eV Light, Curve b.

when the incident light is removed the photocurrent decreases slowly, which shows that a dynamic balance is achieved between filling of the traps optically and releasing of trapped charge carriers thermally. The balance is achieved after about 40 minutes using a 75 watt xenon lamp. These experiments emphasize the importance of the trapping process in the crystal in determining the photoresponse.

Electron-Irradiated Ruby

Electron-irradiation of ruby resulted in a measurable photoresponse only after an optical bleach with 4.4 eV light from a xenon lamp for almost 15 minutes. Figure 17, curves b and c show the photoresponse of the electron-irradiated ruby before and after the 4.4 eV bleach respectively. The band that grew in as a result of the electron-irradiation and 4.4 eV bleach is shown as curve a in Figure 19. This is the difference curve between curves a and c in Figure 17. The peak of the band is at 5.4 eV which appears to correspond to an optical absorption band which Turner and Crawford (4) have assigned to Cr^{2+} . The band appears to be about the same as that for the γ -irradiated ruby except that the decay of the photocurrent occurred slowly over a period of days.

For completeness optical absorption spectra is shown in Figure 18 for electron-irradiated ruby before the 4.4 eV bleach (curve b) and about a week after the bleach (curve c).

Temperature Dependence of Irradiated Ruby

The photoconductivity observed in γ -irradiated ruby is

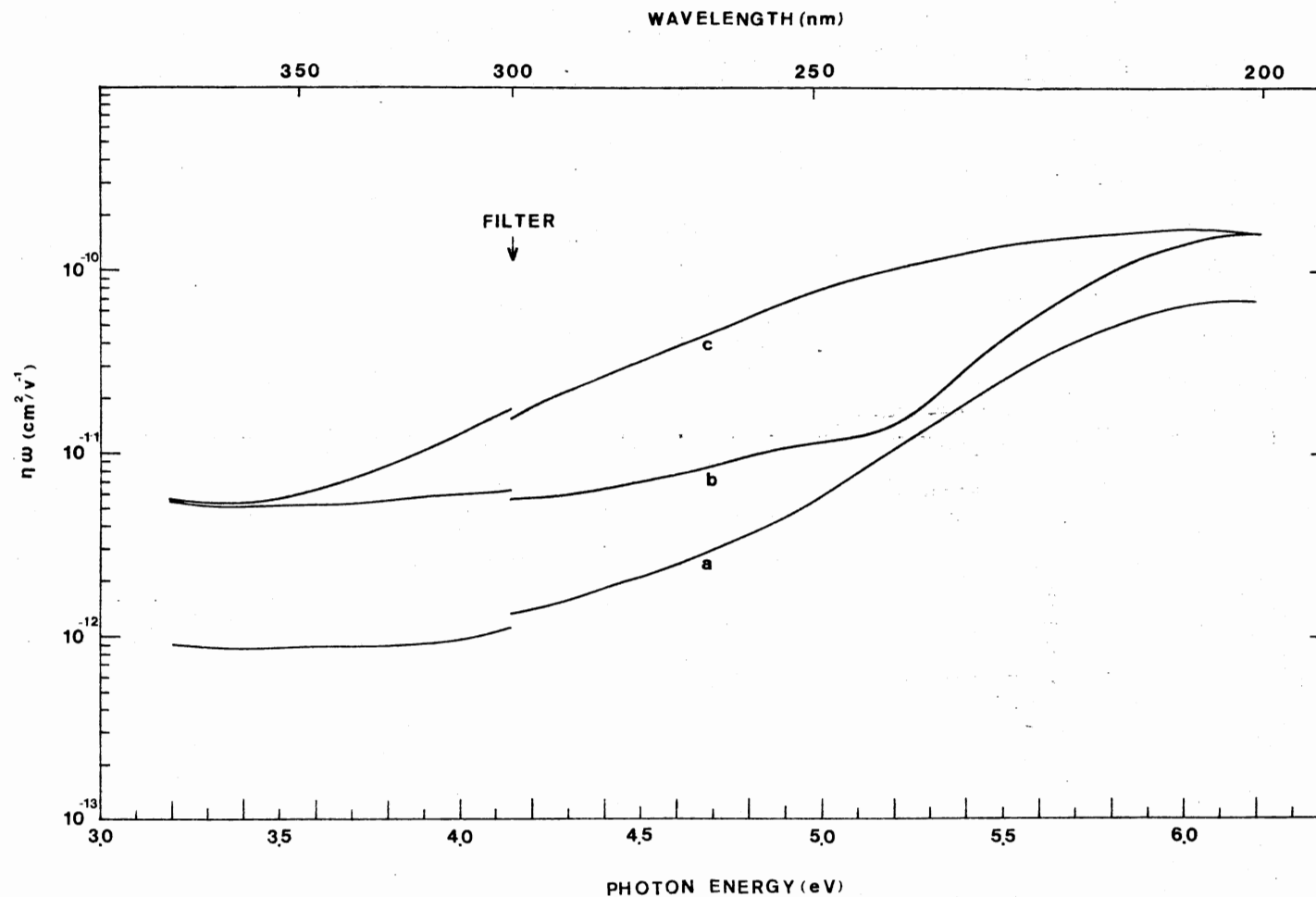


Figure 17. Spectral Dependence of the Photoresponse at Room Temperature of Ruby: Non-Irradiated Sample, Curve a; Electron-Irradiated Sample Irradiated at 77 K with 1.5 mev Electrons to a Dose of about 4.5×10^{16} Electrons/cm², Curve b; the Electron-Irradiated Sample after Bleaching for 15 minutes with 4.4 eV Light at Room Temperature.

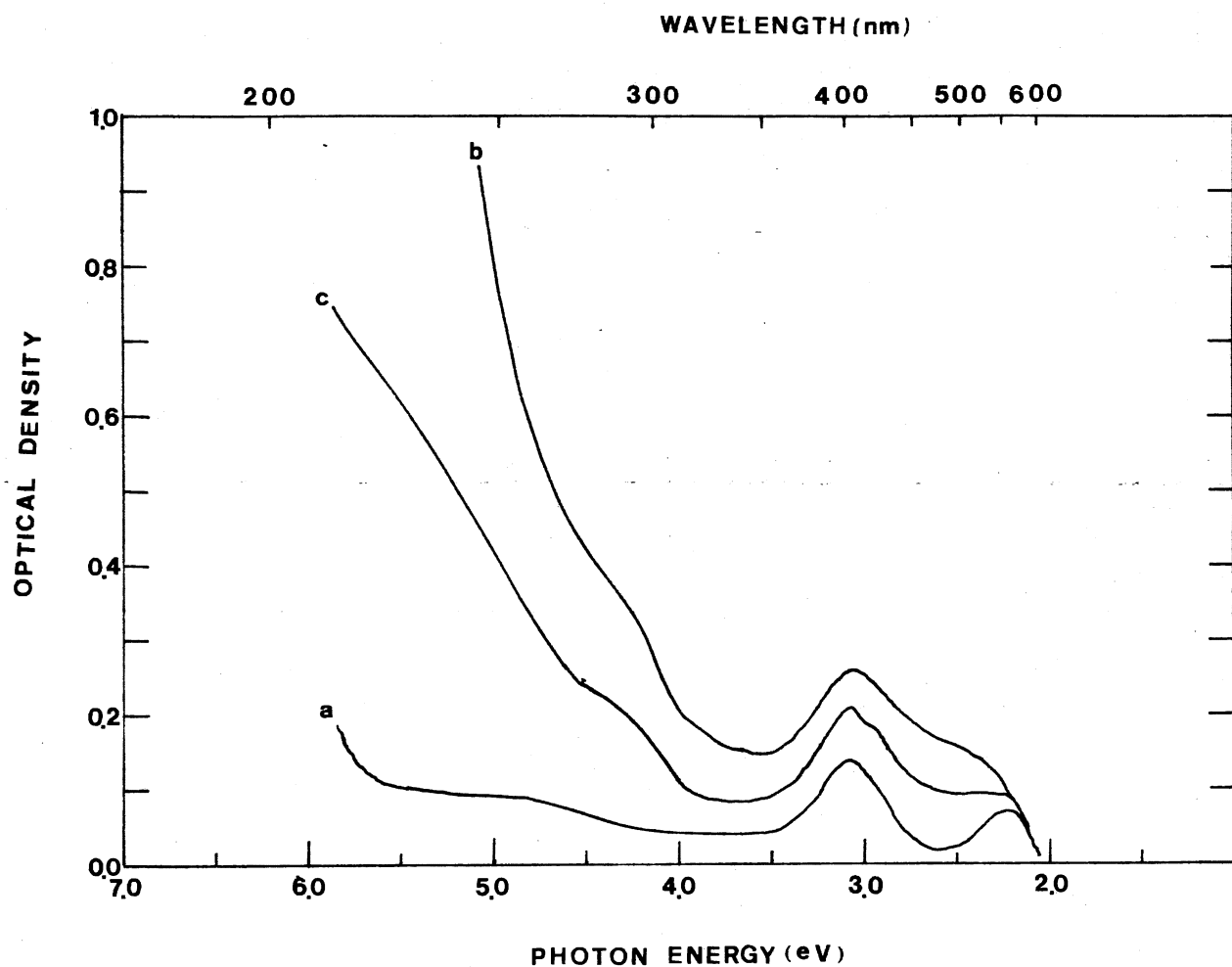


Figure 18. Optical Absorption Spectra at Room Temperature of Ruby: Non-Irradiated Sample, Curve a; Electron-Irradiated Sample Irradiated at 77 K to a Dose of about 4.5×10^{16} Electrons/cm² with 1.5 mev Electrons, Curve b; the Electron-Irradiated Sample after Bleaching at Room Temperature for 15 minutes with 4.4 eV Light, Curve c.

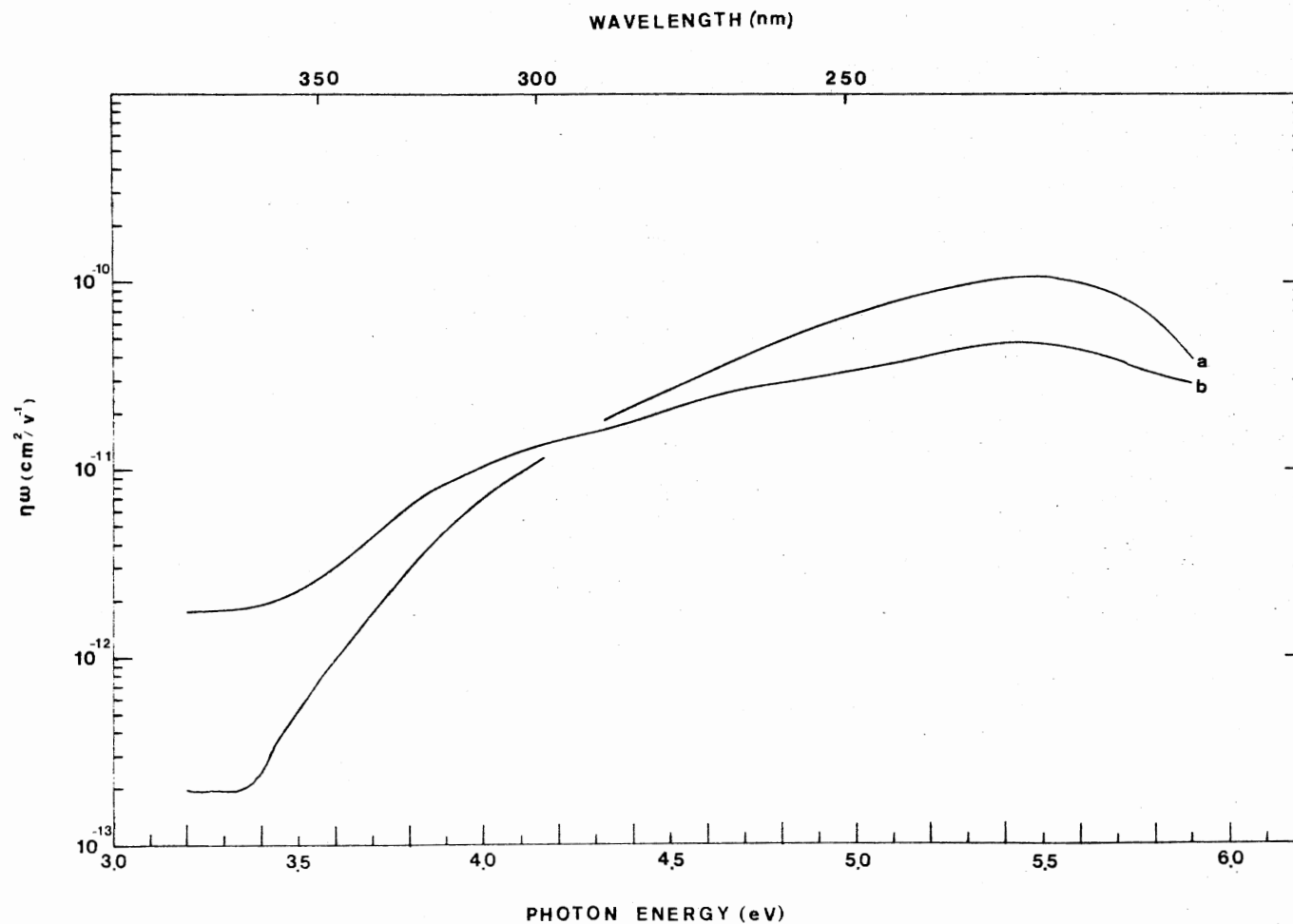


Figure 19. 4.5 eV Photoconductivity Bands as Difference Curves:
 Difference Curve Between Curves a and c of Figure
 13, Curve a; Difference Curve Between Curves a and b
 of Figure 15, Curve b.

markedly temperature dependent. Between 77 K and about 250 K the material shows no photoconductivity. Above 250 K the photoresponse grows rapidly with increasing temperature, which indicates that the photoconductivity was thermally activated. The photoconductivity may grow because of an extension of the carrier range rather than because of an increase in the quantum efficiency for the production on the carriers.

The electron-irradiated sample's photoresponse grew steadily as the temperature varied from 77 K to room temperature, with a small peak occurring at about 3.9 eV between the temperatures of 77 K and 214 K.

An Interesting Insaco Sample

A particularly interesting crystal obtained from Insaco has an optical density similar to a neutron-irradiated Linde sample of Lee and Crawford (1). The Linde sample had optical absorption peaks at 6.1 eV and 4.8 eV. It was shown that the changes of the 6.1 eV band intensity was a linear function of the change in 4.8 eV band absorption when the sample was bleached with either 6.1 eV or 4.8 eV light. Optical bleaching into the 6.1 eV band resulted in a decrease of that band. Similarly bleaching into the 4.8 eV resulted in a decrease of that band. The interpretation of the decrease of the 6.1 eV band and growth of the 4.8 eV band is that bleaching into the 6.1 eV band release an electrons from the F centers converting them to F^+ center. The electrons released must be captured by traps besides the F^+ centers to create the effect otherwise the F^+ would be converted

to an F center and the number of F and F^+ centers would remain unchanged. Calculation of the oscillator strengths, F , of the two bands resulted in the ratio:

$$\frac{f_{6.1}}{f_{4.8}} \sim 2$$

In alkaline earth oxides the oscillator strength ratio of the F center to that of the F^+ center is nearly two. These effects coupled with polarized emission and excitation spectra led Lee and Crawford to suggest that the 6.1 eV and 4.8 eV bands may be due to F and F^+ centers respectively.

The non-irradiated Insaco sample has the same prominent optical peaks as Lee and Crawford neutron-irradiated sample. The optical absorption spectrum for the Insaco crystal is shown as curve a in Figure 20. Curve b in the same figure shows the sample's optical density after being bleached for approximately 30 seconds with light from an unfiltered deuterium lamp. The optical density shows a decrease in the 6.1 eV band by about 7% and an increase in the 4.8 eV band of roughly 30%. The 5.35 band believed to be due to Cr^{2+} also grew as in the neutron-irradiated sample.

In addition the 4.8 eV absorption band in the Insaco sample produced a luminescence band centered at about 3.75 eV which is similar to the luminescence band produced by Lee and Crawford's sample. The luminescence band of Lee and Crawford's sample is shown in Figure 21. The luminescence band of the Insaco sample is shown in Figure 22. The excitation spectrum of the Insaco sample for the 3.75 eV band

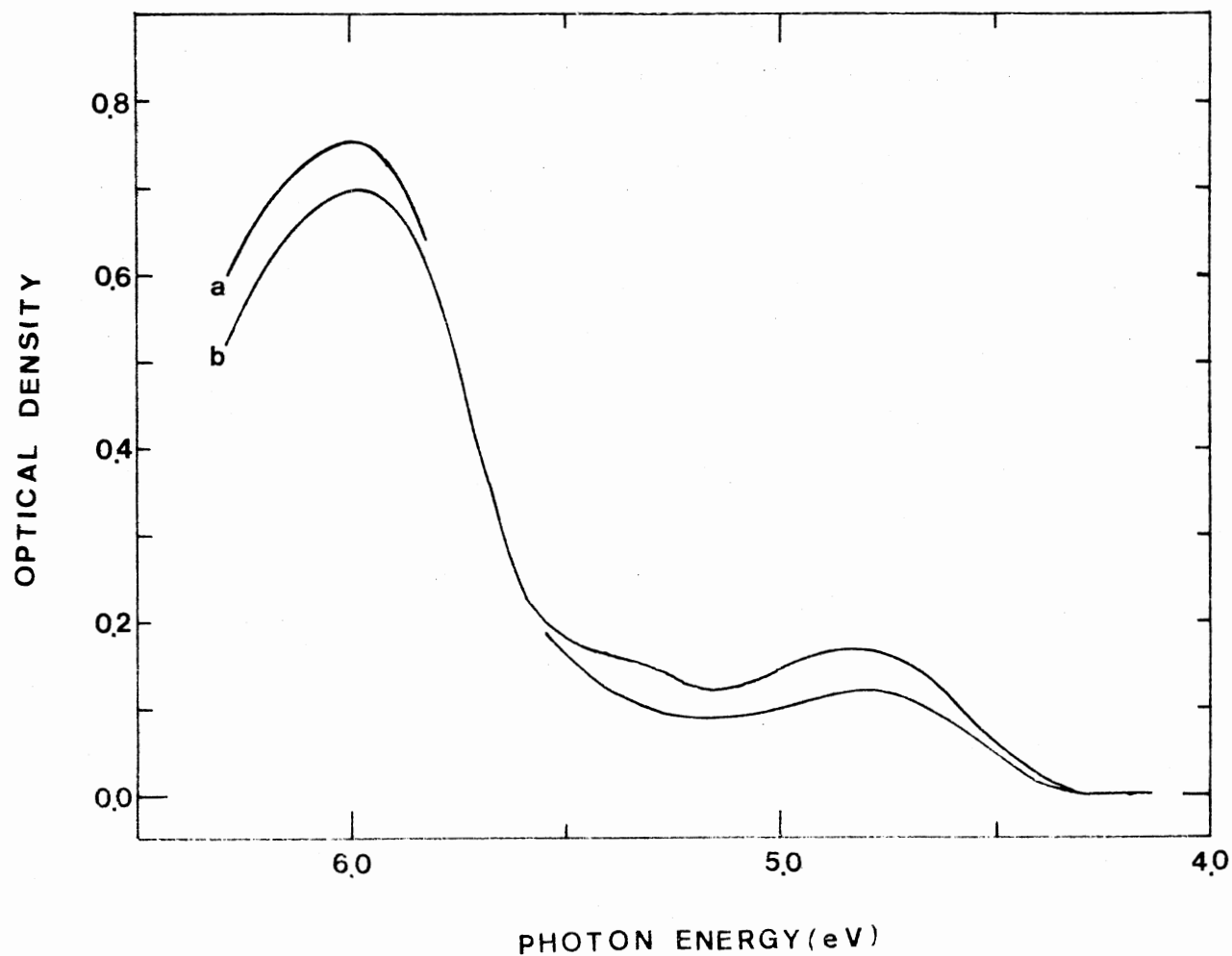


Figure 20. Optical Absorption Spectra at Room Temperature of Insaco Sample: Non-Irradiated Sample, Curve a; the Non-Irradiated Sample after Bleaching for Approximately 30 seconds with Unfiltered Light from a Deuterium Source, Curve b.

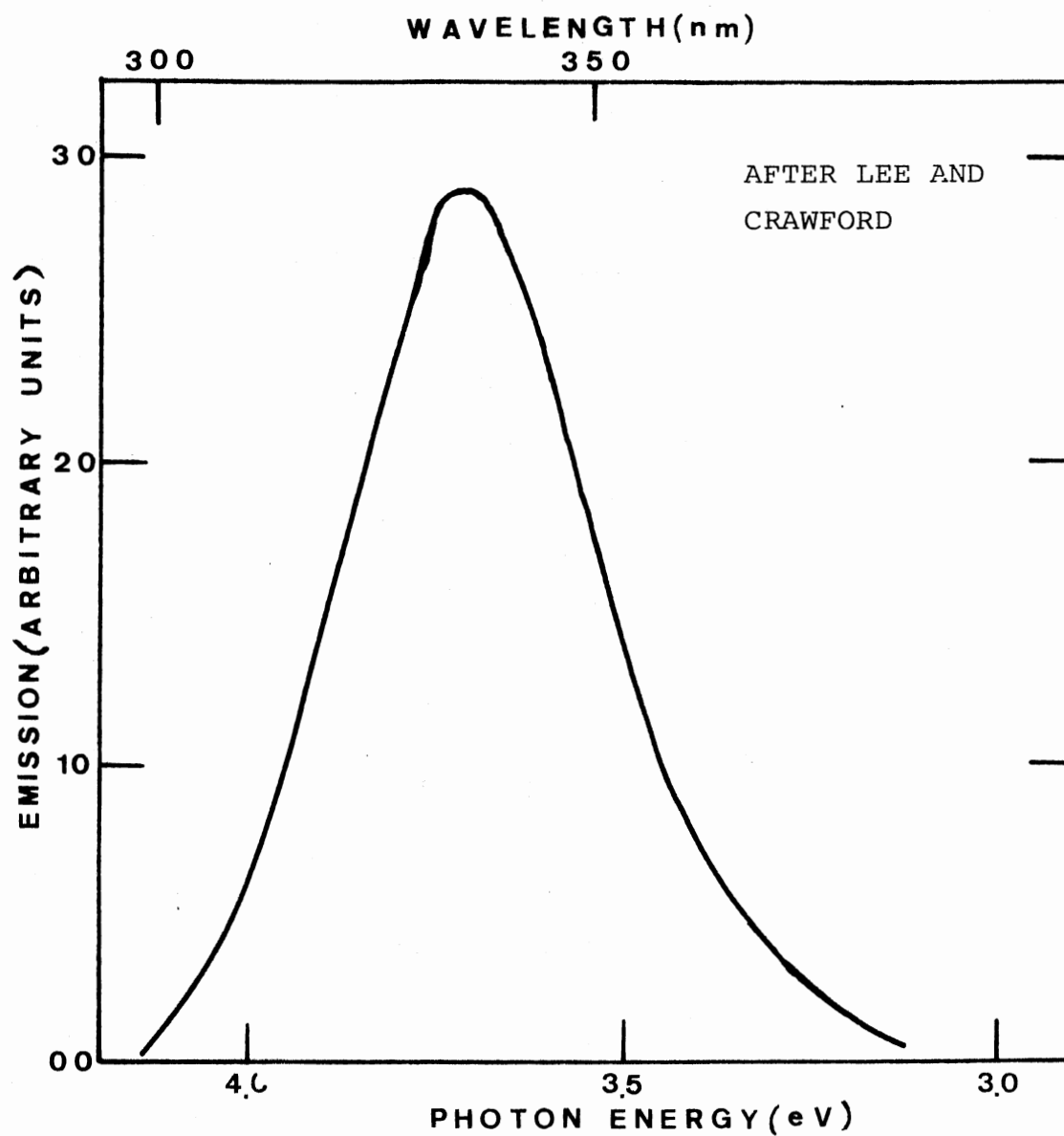


Figure 21. Emission Spectrum of Neutron-Irradiated Al_2O_3 Using 4.8 eV Light as the Exciting Light. The neutron dose was 5×10^{16} neutrons/cm².

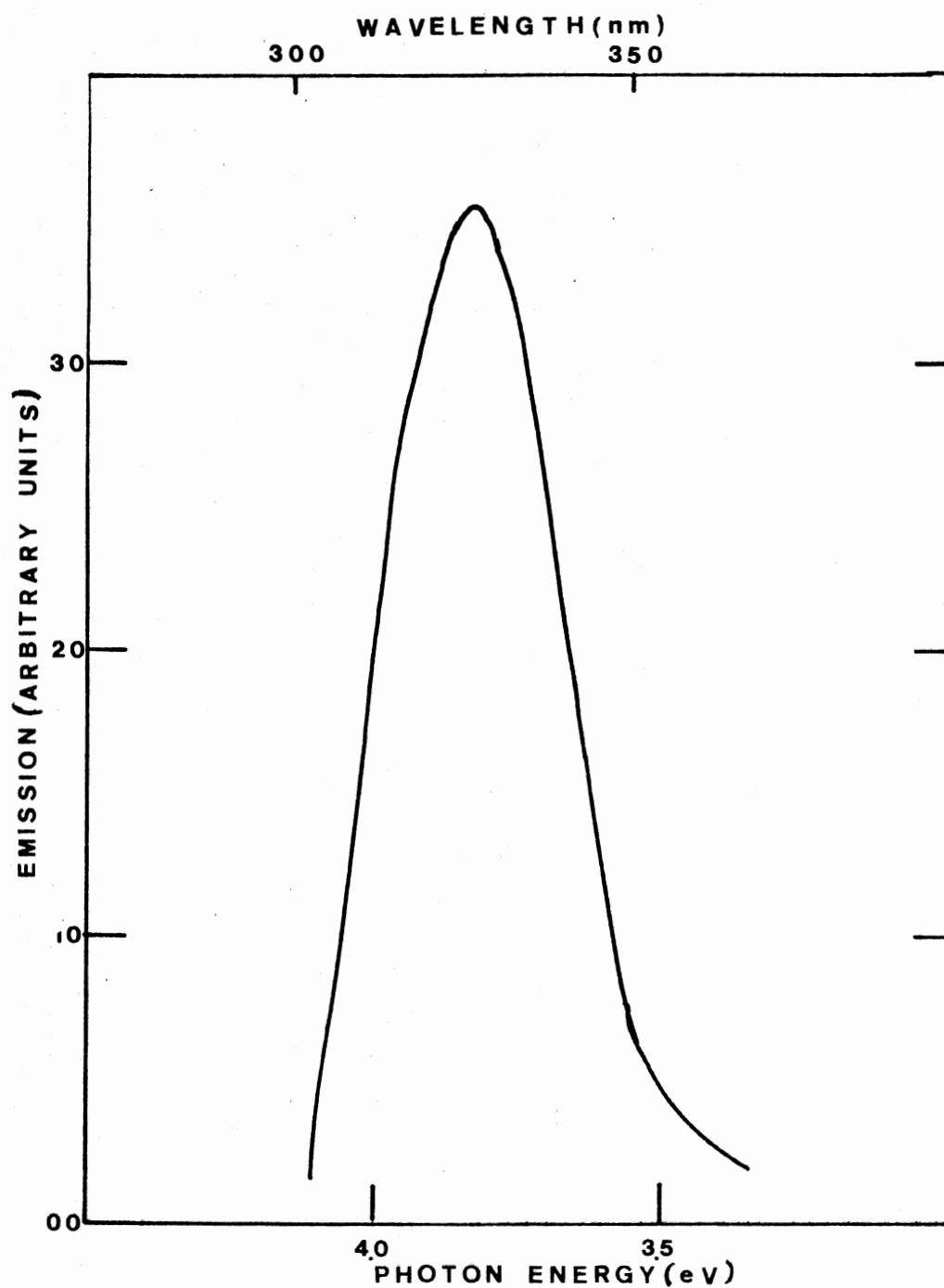


Figure 22. Emission Spectrum at Room Temperature of Non-Irradiated Al_2O_3 Using 4.8 eV Light as the Exciting Light.

showed peaks at 4.8 eV and 5.45 eV.

If Lee and Crawford's conclusions that the 6.1 eV and the 4.8 eV absorption bands are due to F-type centers is correct, then our results indicate that these centers can be produced in sapphire during growth, i.e., sapphire can be accidentally colored in a manner similar to CaO. However, so far attempts at deliberate coloration of sapphire by heating in an atmosphere of aluminum vapor have failed. At this time, then, our results tend to indicate that the correct conditions to additively color sapphire have not yet been found (10).

CHAPTER V

FUTURE

Our understanding of the photoconductivity in aluminum oxide is still preliminary. The results of photoconduction and the optical density on the irradiated and doped crystals must be closely compared with esr results to carefully monitor the charge states of the impurities. The lifetime of the carriers needs to be investigated to give an understanding of the trap depths. Different concentrations and types of dopants need to be studied in Al_2O_3 . The sign of the carriers also need to be found in order to determine the charge states of the impurities.

A SELECTED BIBLIOGRAPHY

1. Lee, K. H., and Crawford Jr., J. H., Phys. Rev. B 15, 4065 (1977).
2. Tippins, H. H., Phys. Rev. B 1, 126 (1970).
3. Lee, R. S., Marrs, C. D., and Merklin, J. F., Bull. Am. Phys. Soc. 22, no. 3, 328 (1977).
4. Turner, T. J., and Crawford Jr., J. H., Solid State Commun. 17, 167 (1975).
5. Klaffky, R. W., and Rose, B. H., Bull. Am. Phys. Soc. 22, 327 (1977).
6. McClure, D. S., Private Commun. (1977).
7. Turner, T. J., and Crawford Jr., J. H., Phys. Rev. B 13, 1735 (1976).
8. Van Heyningen, R. S., and Brown, F. C., Phys. Rev. B 3, 462 (1958).
9. Hecht, K., Z. Physik 77,235 (1932).
10. Chen, Y., Private Commun. (1977).

VITA

Billy Gene Draeger, Jr.

Candidate for the Degree of

Master of Science

Thesis: PHOTOCODUCTIVITY AND LUMINESCENCE IN Al_2O_3

Major Field: Physics

Biographical:

Personal Data: Born in Chelsea, Oklahoma, August 16, 1950, the son of Mr. and Mrs. F. D. Hall.

Education: Graduated from Wynona High School, Wynona, Oklahoma, in May, 1968; received Bachelor of Science degree in Physics from Oklahoma State University in 1975; completed requirements for the Master of Science at Oklahoma State University in July, 1977.